2019/2020 RENOURISHMENT PROJECT
OAK ISLAND, NORTH CAROLINA

JAY BIRD SHOALS BORROW AREA MODELING

Prepared for:

Town of Oak Island

Prepared by:

moffatt & nichol

2019/2020 RENOURISHMENT PROJECT
OAK ISLAND, NORTH CAROLINA

# JAY BIRD SHOALS BORROW AREA MODELING

M&N Project No.10128-01

Revision	Description	Issued Date	Author	Reviewed	Approved
A	Modeling report	September 6, 2019	ZW	KF	JM

moffatt & nichol

EXECUTIVE SUMMARY

In order to investigate the potential effects of dredging material from a Jay Bird Shoals borrow area identified for the 2019/2020 Renourishment Project on neighboring shorelines of Caswell Beach and Bald Head Island, numerical models were developed to investigate hydrodynamics, waves, and sediment transport using Deltares' Delft3D model suite. The hydrodynamics and wave models were successfully calibrated and validated against available observed water levels, currents, discharges, and wave data. The sediment transport model was not calibrated due to lack of measured data to calibrate against.

Tidal current, wave, and sediment transport modeling was performed for the existing and after-dredge bathymetry scenarios. Two borrow area after-dredge templates were considered. Template 1 was designed to dredge 2.95 million cubic yards (mcy) and Template 2 was designed to dredge 2.34 mcy of available beach compatible material. For both after-dredge templates only part of the material, 1.1 mcy, will be dredged for the 2019/2020 Renourishment Project. Thus, within the proposed borrow area, the results from the Delft3D model are believed to be a conservative overestimate of the potential effects on the tidal current and wave climates.

The tidal current model results indicate that for both after-dredge bathymetry templates effects on residual tidal currents would be localized and small. This implies there would be no significant effects on sediment transport processes associated with tidal currents. The figure below shows the effects of the two after-dredge bathymetry templates on residual tidal currents over a spring-neap tidal cycle.
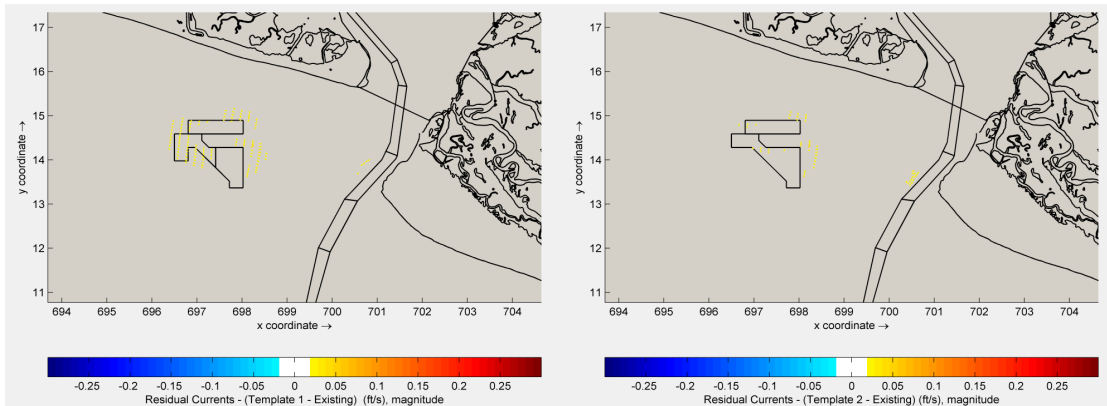
After-dredge bathymetry effects on residual tidal currents over a spring-neap tidal cycle

The wave transformation model results for the 2004 – 2018 average annual offshore wave climates show that the two after-dredge bathymetry templates could result in a slight redistribution of wave energy along the shoreline during moderate to severe storm events.

Sediment transport modeling was also completed, to observe if the changes to wave heights and wave directions would affect the longshore transport. The sediment transport modeling results for both after-dredge bathymetry templates show that the wave-induced longshore sediment transports could be reduced leeward of the borrow area but could potentially increase on shoreline segments both east and west sides of the borrow area. The net effect of these changes could result in localized adjustments in shoreline erosion / accretion. Based on the model results of the longshore sediment transport gradients as presented below, most of the potential increases in shoreline erosion would be limited to discrete portions of Caswell Beach (between survey transects 37+00 –60+00 and 150+00 – 170+00). Generally, both templates show results close to existing conditions, with some areas above and below existing. There is no strong evidence to choose one template over the other given the model results, especially given that this is not a morphological model. The modeled sediment transport inside the surf zone is greatly influenced by the imposed model bathymetry. Thus, the model results only represent the bathymetric condition constructed based on the available data sources. There will be an additional 0.6 mcy beach compatible material available in Template 1. For this reason, Template 1 was chosen for the Town of Oak Island's permit application for the 2019/2020 Renourishment Project. The Town of Oak Island will monitor the Caswell Beach shoreline for nine (9) years post-project to investigate any potential effects which might require mitigation.

Wave-induced longshore sediment transport gradients along Caswell Beach shoreline

TABLE OF CONTENTS

LIST OF FIGURES

LIST OF TABLES

1.   INTRODUCTION

Moffatt & Nichol was retained by the Town of Oak Island for professional services to execute the 2019/2020 Renourishment Project following Hurricane Matthew.

The Jay Bird Shoals borrow area shown in Figure 1-1 was identified as a potential borrow area for this beach renourishment project. In order to determine if potential adverse effects to the neighboring Caswell Beach and Bald Head Island shorelines could be a possibility, numerical modeling studies were conducted.

Delft3D, an open-source, fully integrated numerical modeling suite developed by Deltares, Netherland, was selected as the modeling platform. Delft3D can carry out numerical modeling of flows, waves, sediment transport, morphological developments, water quality and ecology in coastal, river, lake and estuarine areas.   For the purpose of this study, two modules in Delft3D were used: Delft3D-FLOW (Deltares, 2018a) and Delft3D-WAVE (Deltares, 2018b). Delft3D-FLOW is the hydrodynamics and sediment transport module; whereas Delft3D-WAVE is the wave transformation module.

In this report, the effects of dredging material from a borrow area in Jay Bird Shoals on waves, tidal current velocities, and sediment transport patterns were investigated.
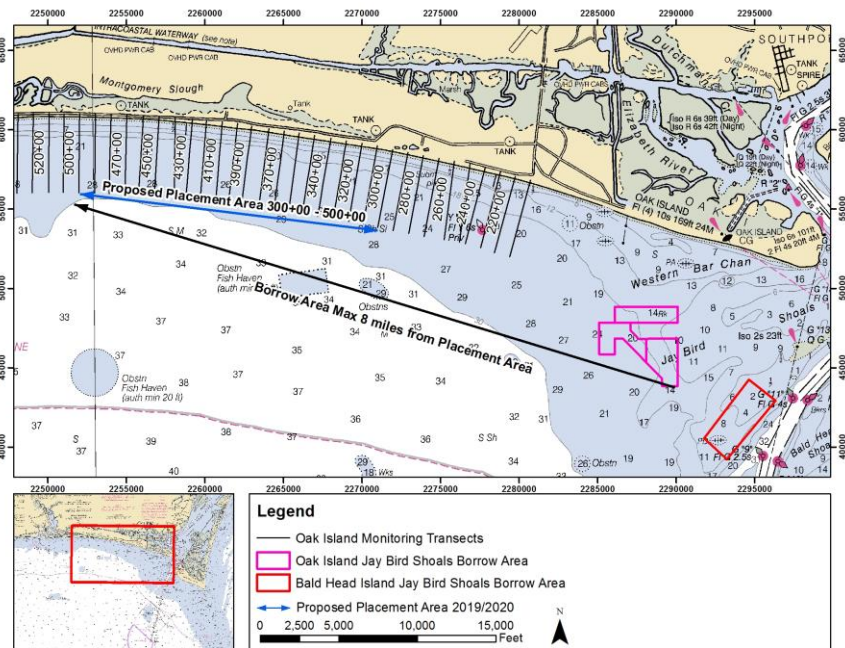
Figure 1-1:   Jay Bird Shoals borrow area

2.   MODEL DEVELOPMENTS

In this section, the developments of flow and wave model grids and bathymetries are discussed. The model horizontal coordinate is in North Carolina State Plane, and the vertical datum is North American Vertical Datum (NAVD88).

2.1   MODEL GRIDS

2.1.1   Flow Model Grids

The flow model domain included the Cape Fear River estuary from upstream of the Cape Fear, Black, and Northeast Cape Fear Rivers to 20 miles offshore from the mouth of Cape Fear River near Southport, NC. The grid cell sizes were variable throughout the domain. In the offshore area the resolution was approximately 90 meters. For the upstream Cape Fear, Black, and Northeast Cape Fear River areas, the resolution was approximately 30 meters. Along the channel the resolution was approximately five meters. Figure 2-1 presents the flow model grid.
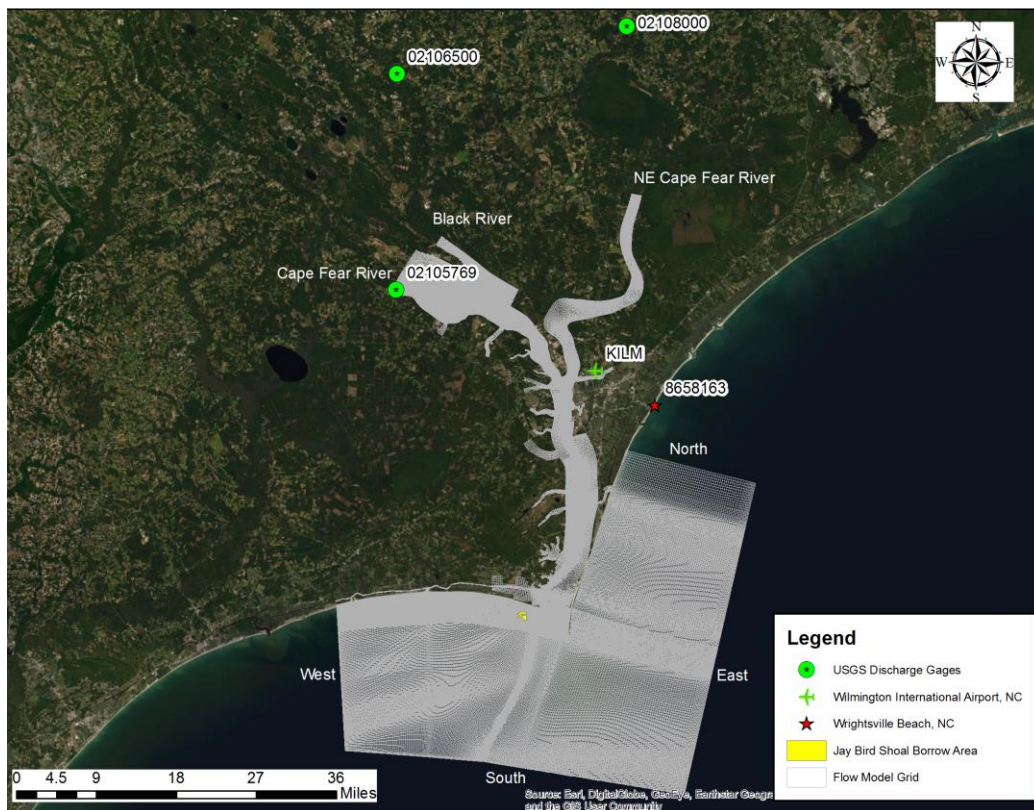
Figure 2-1:   Flow model grid

2.1.2   Wave Model Grids

Wave transformation from deep water to the shoreline was accomplished by nesting three increasingly resolved model domains as shown in Figure 2-2.

The coarsest grid (gray) is comprised of approximately 20,000 cells with size of 500 m x 500 m. The offshore limit of the coarse grid is near the location of the National Oceanic and Atmospheric Administration (NOAA) wave buoy 41013 from which offshore wave conditions were derived.

The medium-resolved wave domain (blue) and the fine wave domain (red) were developed based on the flow model grid. The fine wave model grid has approximately 5-meter cross-shore resolution in the surf zone region of Caswell Beach.
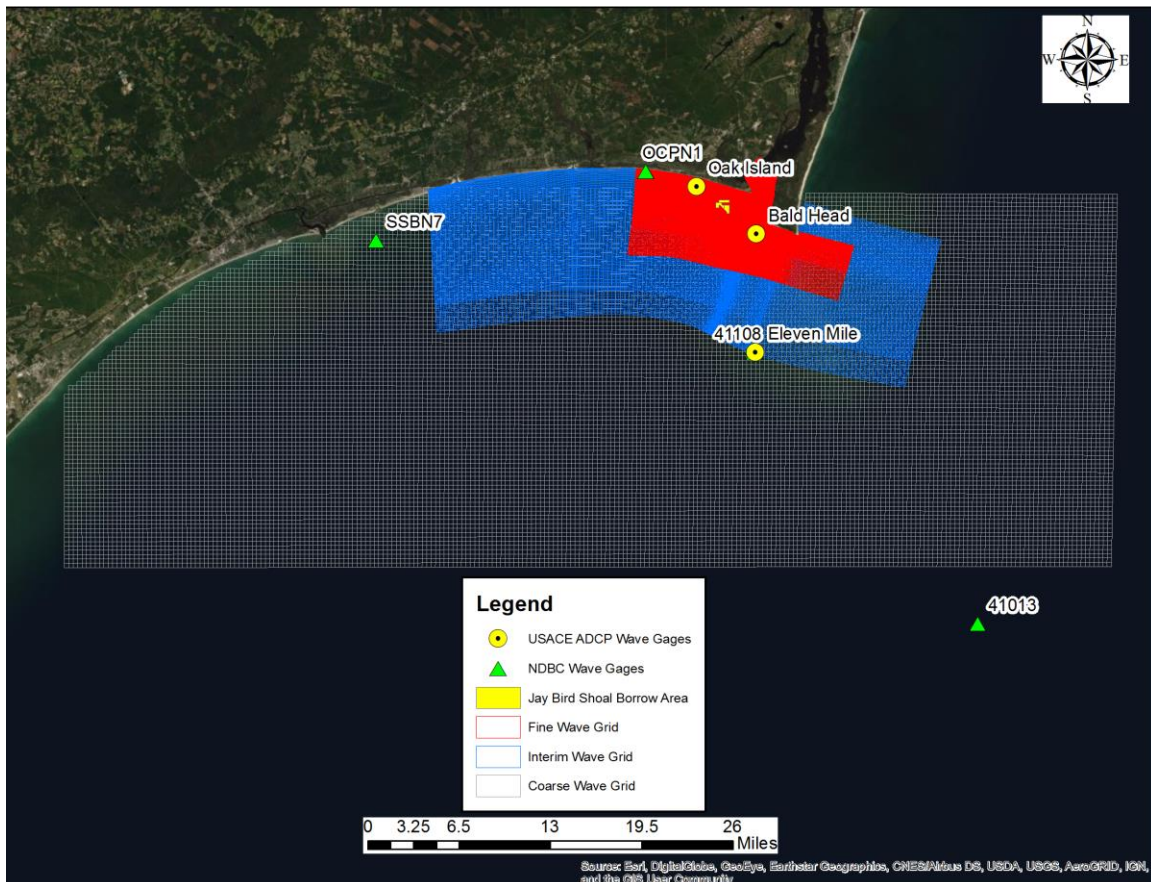
Figure 2-2:   Wave model grids

2.2   MODEL BATHYMETRY

Bathymetric data from different sources were compiled and processed to cover the entire computational domains. All bathymetric datasets were adjusted to NAVD88. The data sources used for the development of the morphology model bathymetry are listed in Table 2-1 from high priority to low priority. The most recent bathymetry data were selected where available to create the model bathymetry.

The terminal groin constructed on the western tip of South Beach on Bald Head Island between June and December 2015 was also included in the model.

Figure 2-3 and Figure 2-4 show the flow model bathymetry and the fine wave model bathymetry under existing conditions, respectively.

Table 2-1:   Model bathymetry data sources

Data Set	Source
Wilmington Harbor hydrographic surveys	USACE 2016 – 2017
Fugro channel bank surveys	Fugro 2016 – 2017
Oak Island post Matthew beach profile surveys (STA 210+00 – 700+00)	TI Coastal 2016
Bald Head Island beach profile surveys (STA 000+00 – 238+00)	USACE 2013
Oak Island beach profile surveys (STA 005+00 – 210+00)	USACE 2012
Cape Fear River 2010 surveys	USACE 2010
NOAA hydrographic surveys	NOAA 1973 – 2007
NOAA Navigation Charts	MIKE C-MAP
ADCIRC bathymetry	NCDPS 2011
NC LiDAR	NOAA 2014 – 2016
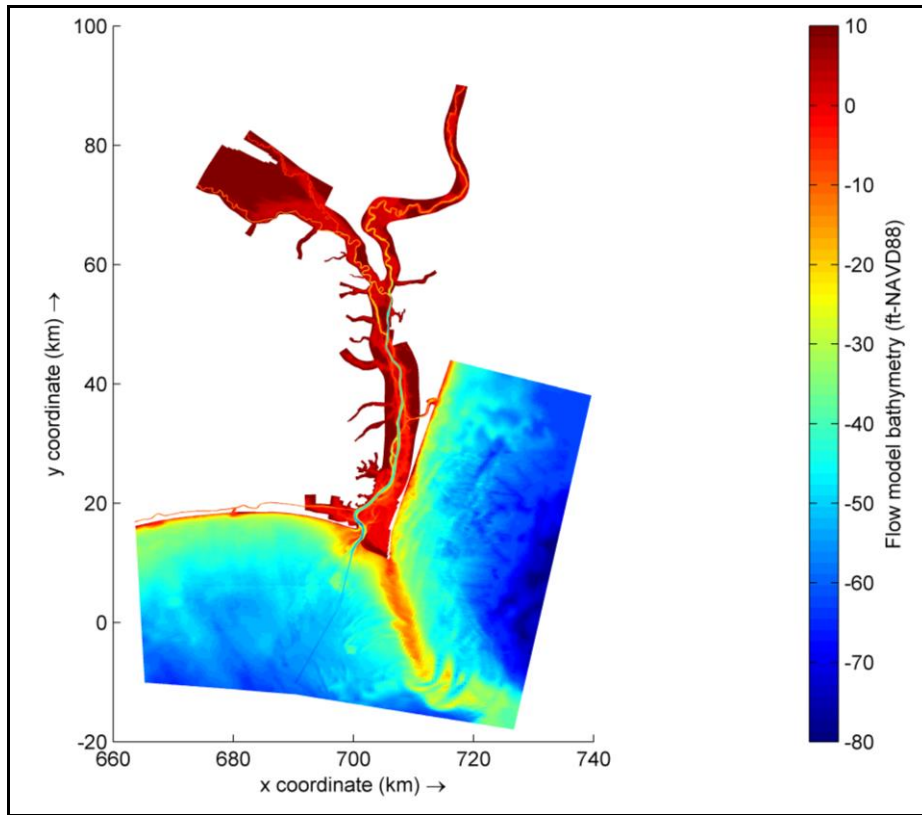
Figure 2-3:   Flow model bathymetry under existing conditions
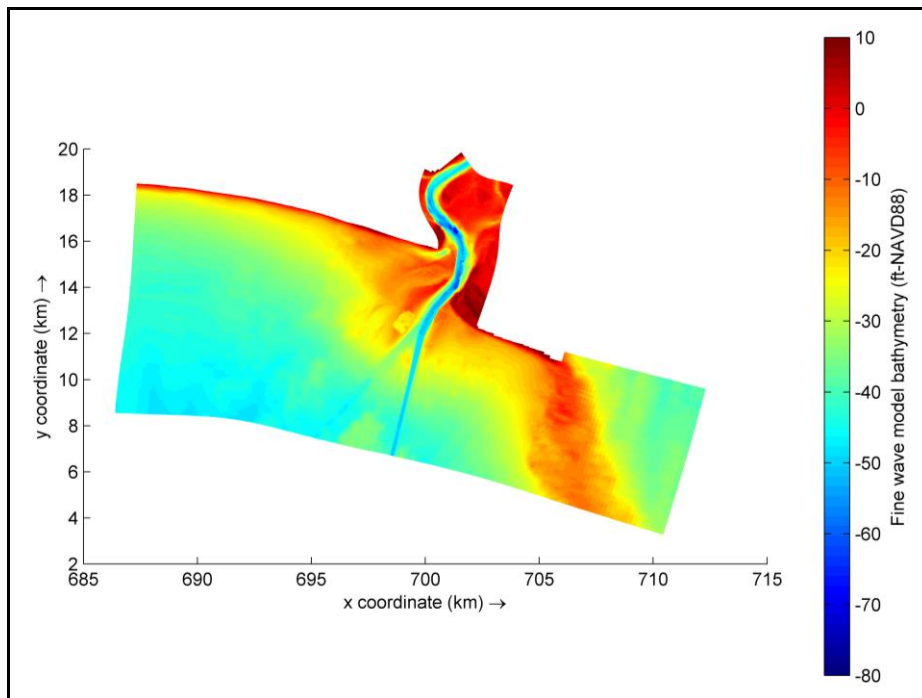
Figure 2-4:   Fine wave model bathymetry under existing conditions

3. MODEL CALIBRATIONS

3.1 CALIBRATION METRICS

Several goodness-of-fit statistical parameters were used to assess model calibration and validation results. These include the mean error (*ME*), root mean square (*RMS*) error, normalized *RMS* error, mean absolute error (*MAE*), correlation coefficient (*R*), index of agreement (*d*), and time delay or lag (Δ*T*). These parameters are briefly described here.

If *x* and *y* are the measured and calculated data respectively, then the following statistics can be calculated:

Mean error (*ME*):

$$ME = \bar{y} - \bar{x} \tag{1}$$

Where "bar" denotes the sample mean.

Root mean square (*RMS*) error:

$$\varepsilon_{RMS} = \sqrt{\overline{(x-y)^2}} \tag{2}$$

To reduce the effect of measurement error and possible outliers, a one-hour low-pass filter was applied to the measured data to compute trend x_f. Then the normalized error is calculated as

$$\varepsilon_{norm} = \frac{\varepsilon_{RMS}}{x_{f,max} - x_{f,min}} \cdot 100\% \tag{3}$$

Where $x_{f,max}$ and $x_{f,min}$ are the maximum and minimum values of the trend x_f. The residual in the denominator defines the range of measured data.

The root mean square error of measured data was estimated as:

$$\varepsilon_{meas} = \sqrt{\overline{(x-x_f)^2}} \tag{4}$$

Mean absolute error (*MAE*):

$$MAE = \overline{|x-y|} \tag{5}$$

The correlation coefficient *R* was calculated using standard method and represents a non-squared value.

The model prediction capability was estimated with an index of agreement between measured and calculated data (Willmott et al., 1985):

$$d = 1 - \frac{\overline{(x-y)^2}}{\overline{\left(|x-\bar{x}| - |y-\bar{x}|\right)^2}}, 0 \leq d \leq 1 \qquad (6)$$

The time delay ΔT shows expected time difference between corresponding events in measured and calculated data. To estimate the delay, the cross-correlation function between measured and calculated data is computed and the smallest time lag at which a maximum occurs is found. Because the cross-correlation function is calculated from discrete data, resulting time resolution may not be sufficient to accurately define the maximum. Therefore, computed values of the cross-correlation function were interpolated with a piecewise polynomial of 5th order, which was then used to determine the maximum.

3.2 FLOW MODEL CALIBRATION

The flow model was calibrated for the period between March 27, 2017 and April 5, 2017 when RPS Evans-Hamilton (RPS EH) conducted water level, current, discharge, salinity, and water quality measurements on the Cape Fear River (RPS Evans-Hamilton, 2017). For the calibration period, water level measurements were available at Southport and Wilmington (Figure 3-1); current measurements were available at Southport (Figure 3-1); and discharge measurements were available at the 11 transects between Wilmington and Southport (Figure 3-2 through Figure 3-5). The model was calibrated to match the measured water levels, discharges, and currents.
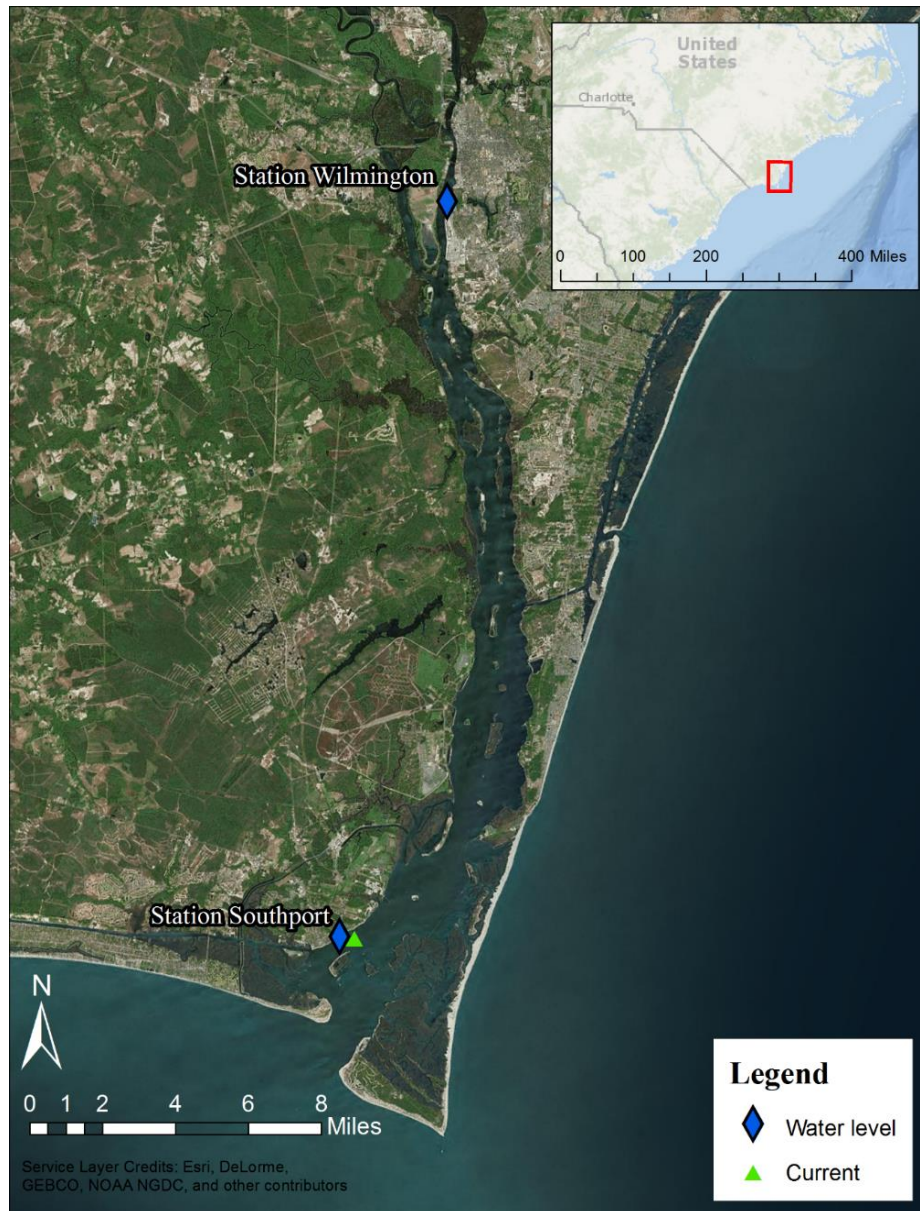
Figure 3-1: **Locations of water levels and current measurements by RPS EH**

Figure 3-2: **Survey transects in Upper Wilmington area by RPS EH**

Figure 3-3:   Survey transects in Lower Wilmington area by RPS EH

Figure 3-4:   Survey transects in Snow's Cut area by RPS EH
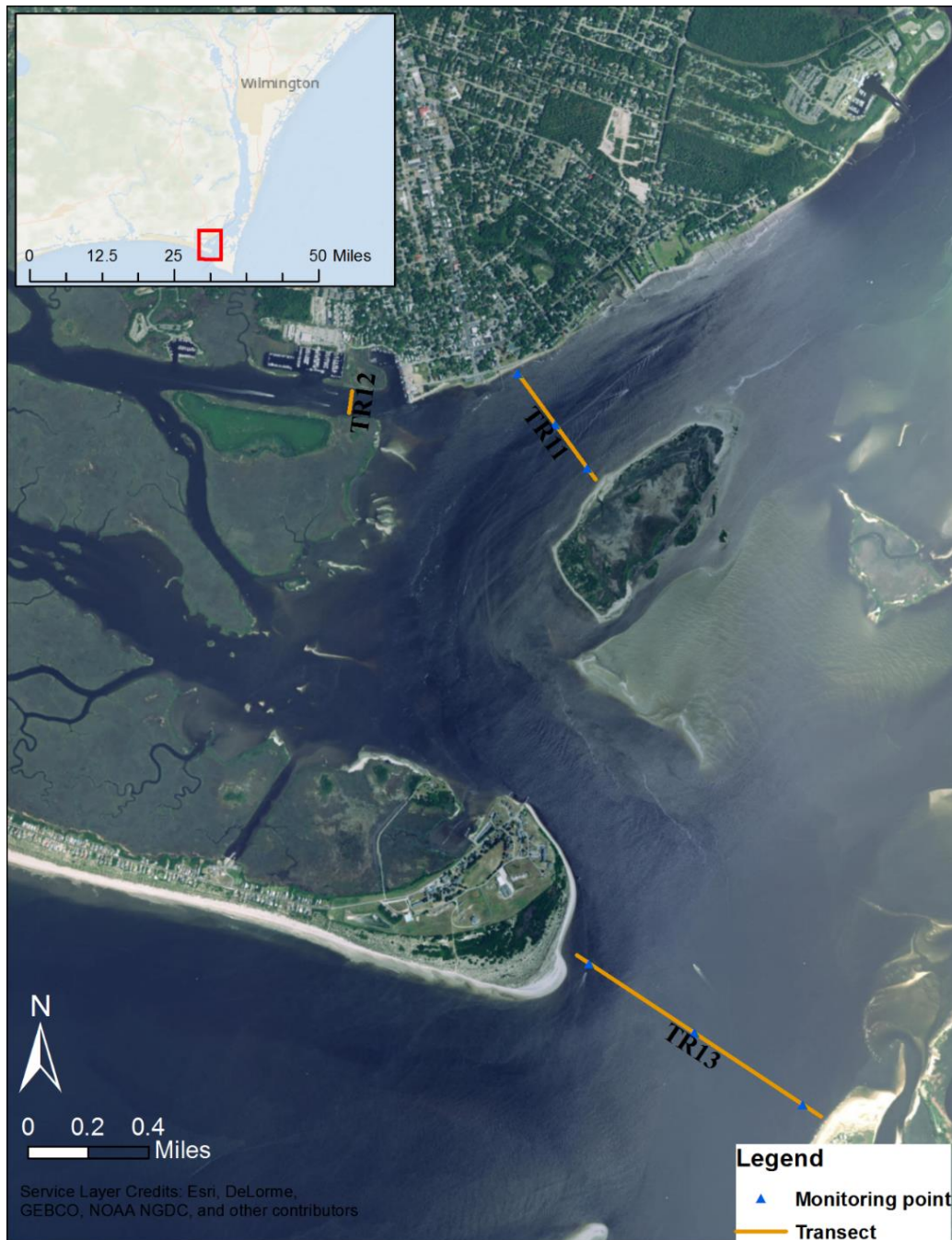
Figure 3-5:   Survey transects in Southport area by RPS EH

3.2.1   Boundary Conditions

The model has seven open boundaries as indicated on Figure 2-1: four offshore – West, South, East, and North; and three upstream – NE Cape Fear River, Black River, and Cape Fear River. The model was forced using tidal water levels at the offshore boundaries

and river discharges at the upstream boundaries. Winds were applied uniformly over the entire domain.

(A)   TIDAL BOUNDARY CONDITIONS

Astronomical tidal constituents for water levels were extracted from the Oregon State University tidal database which is based on TOPEX/Poseidon satellite altimetry data (Egbert and Erofeeva, 2002). The global model with a resolution of 1/6° along with high resolution along coastal areas was used. North and West open boundary were specified as Neumann boundaries, and South and East open boundary were specified as water level boundaries.

(B)   RIVER DISCHARGES

The time series of discharges from the rivers measured at three United States Geological Survey (USGS) stations (shown in Figure 2-1) were used at the three upstream open boundaries: discharge data at Station 02105769 was used at the upstream boundary at the Cape Fear River, Station 02106500 data was used at the Black River, and Station 02108000 data was used at the Northeast Cape Fear River.   The discharges from the un-gaged drainage areas between the USGS stations and the model upstream boundaries were accounted for with appropriate scale factors based on the ratio of un-gaged drainage area vs. gaged drainage area for each branch.

(C)   WINDS

From the analysis of available wind data, it was found that the wind field in the Cape Fear River estuary is very seasonal in nature, i.e., predominant wind direction changes according to the season, and wind speeds vary depending on the location of the station. Stations that are offshore indicate higher wind speed than stations located on the coast or on land.

Wind data from Station KILM (Wilmington International Airport) shown in Figure 2-1 was used to force the model. Station KILM is located on the land and is considered to better represent wind over the estuary compared to the offshore stations.

3.2.2   Calibration Results

Water levels, currents, and discharges obtained from the model results were compared with measurements available at various locations. Figure 3-6 shows the comparison of

water level time series. It can be seen that the model replicates the water levels well with a small over prediction for most of the time (Station Wilmington (NOAA)). Figure 3-7 shows the comparison of depth-averaged currents and the model also replicates the currents at Southport well.

Figure 3-8 through Figure 3-12 show comparisons of the discharge measurements. The statistics shown in those figures were calculated by comparing the model and measurement values at corresponding times. The positive and negative discharge correspond to ebb current and flood current direction, respectively. The calibration results match well at all transects in the main channel.
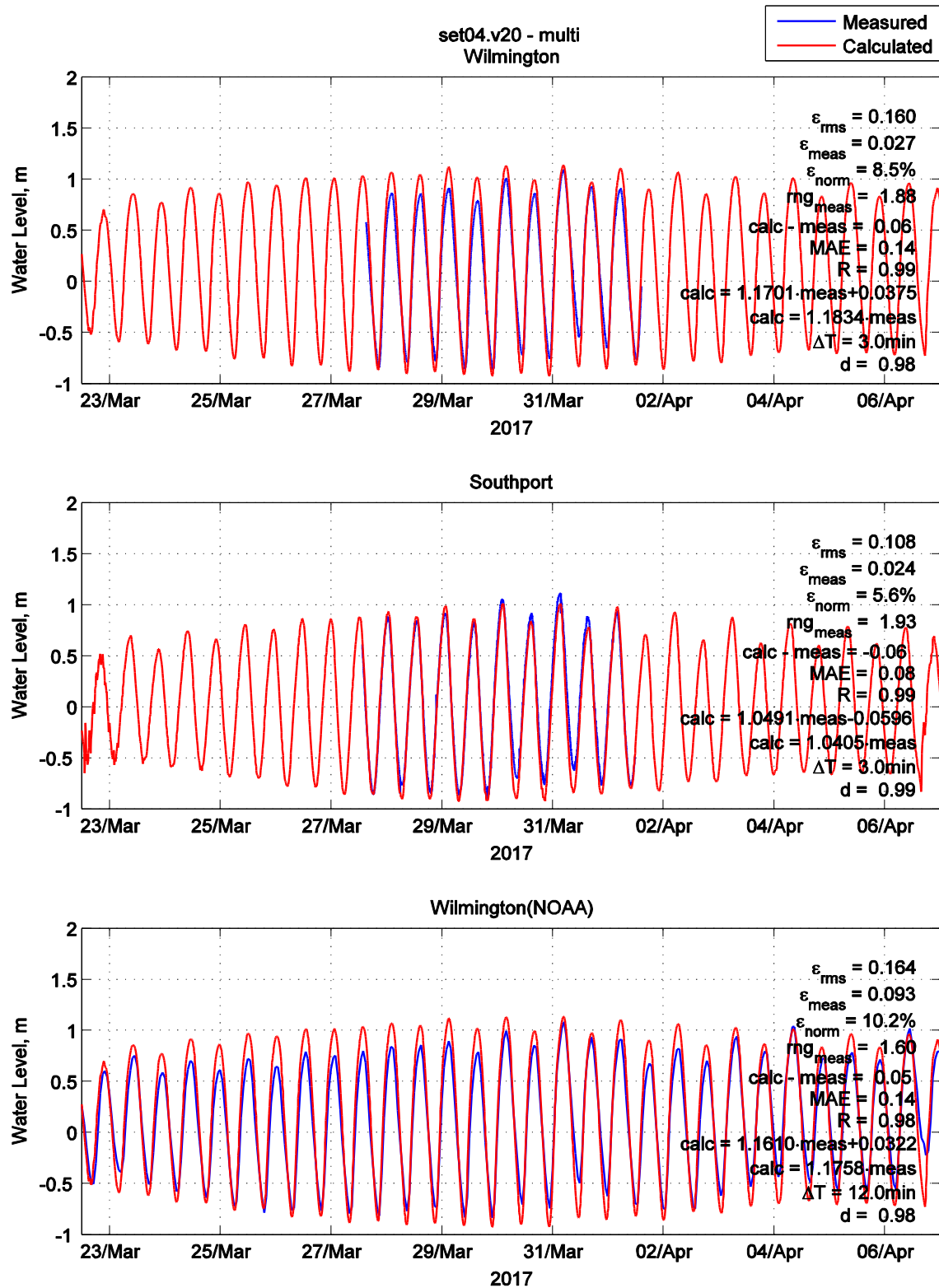
Figure 3-6:   Water level calibration results
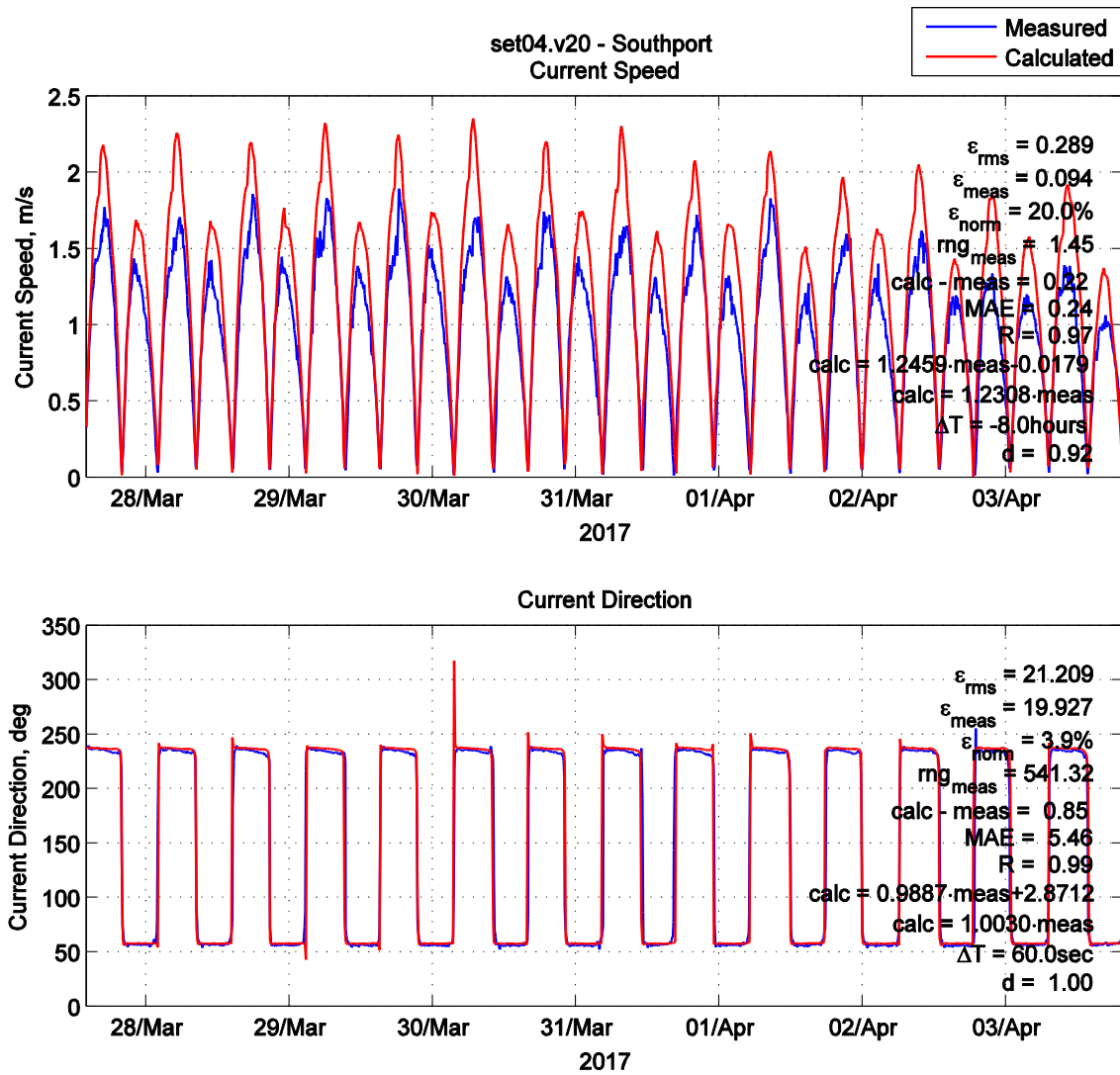
Figure 3-7: Depth-averaged current calibration results
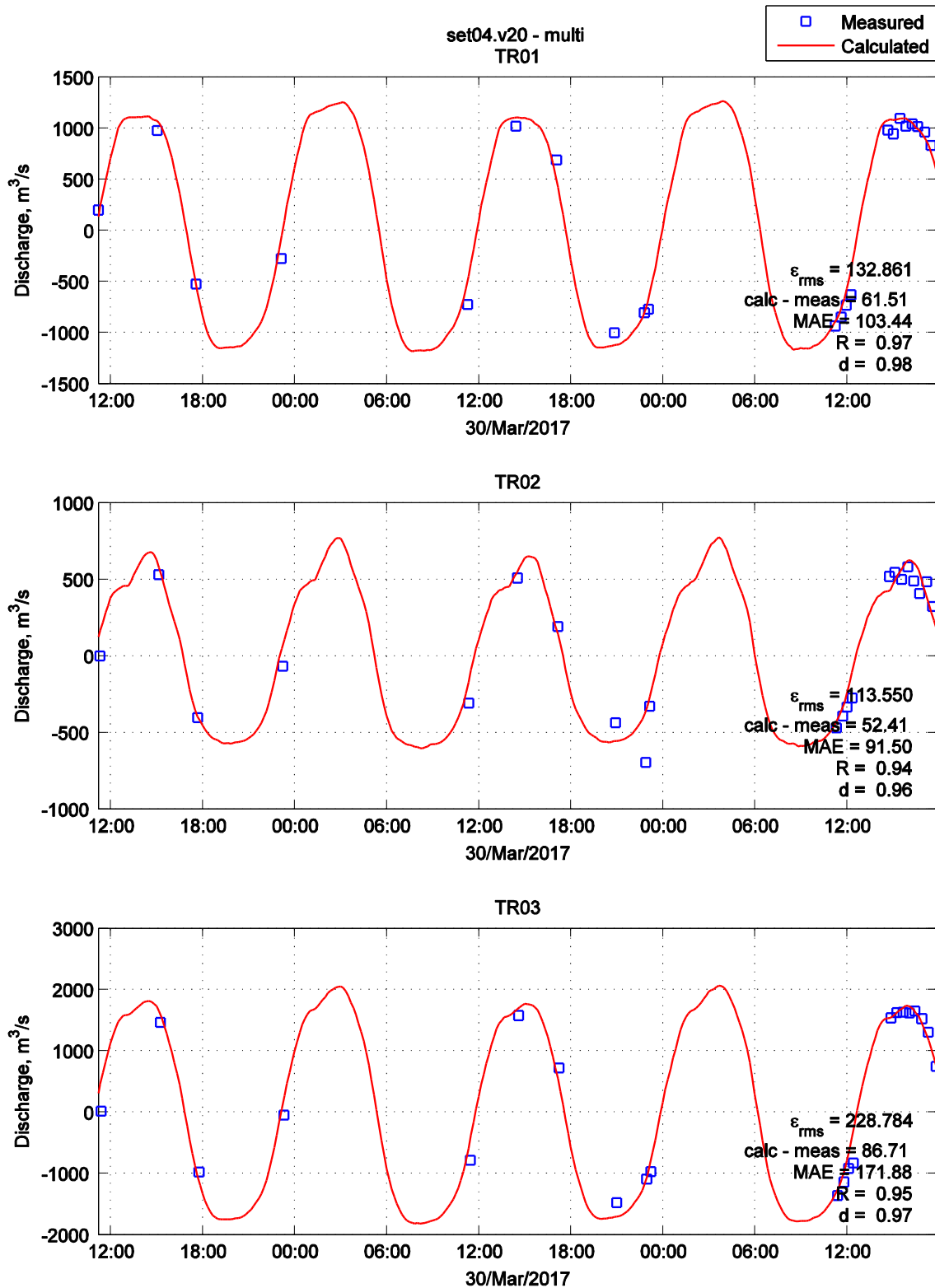
Figure 3-8:   Discharge calibration results (TR01 – TR03)
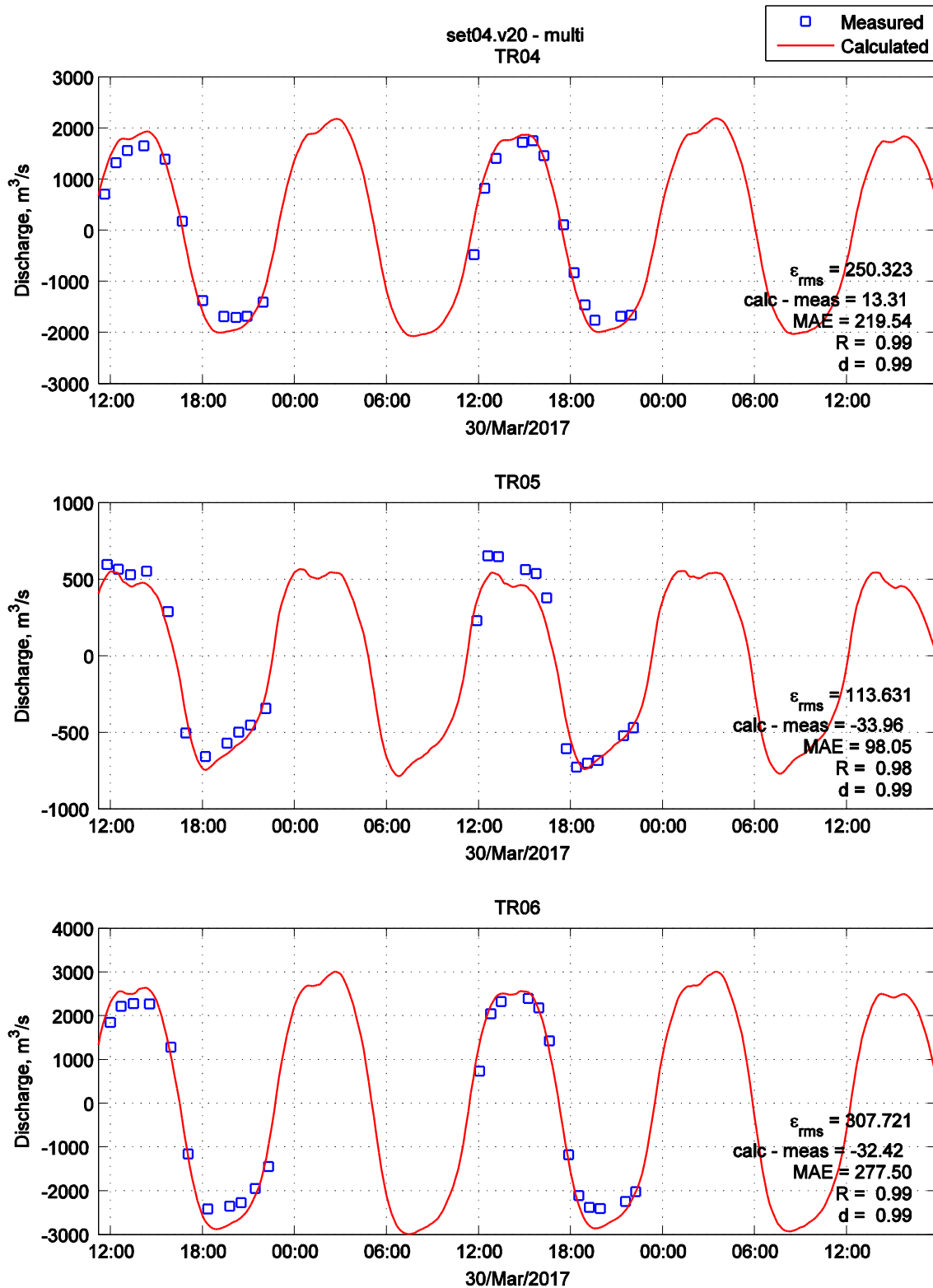
Figure 3-9:   Discharge calibration results (TR04 – TR06)
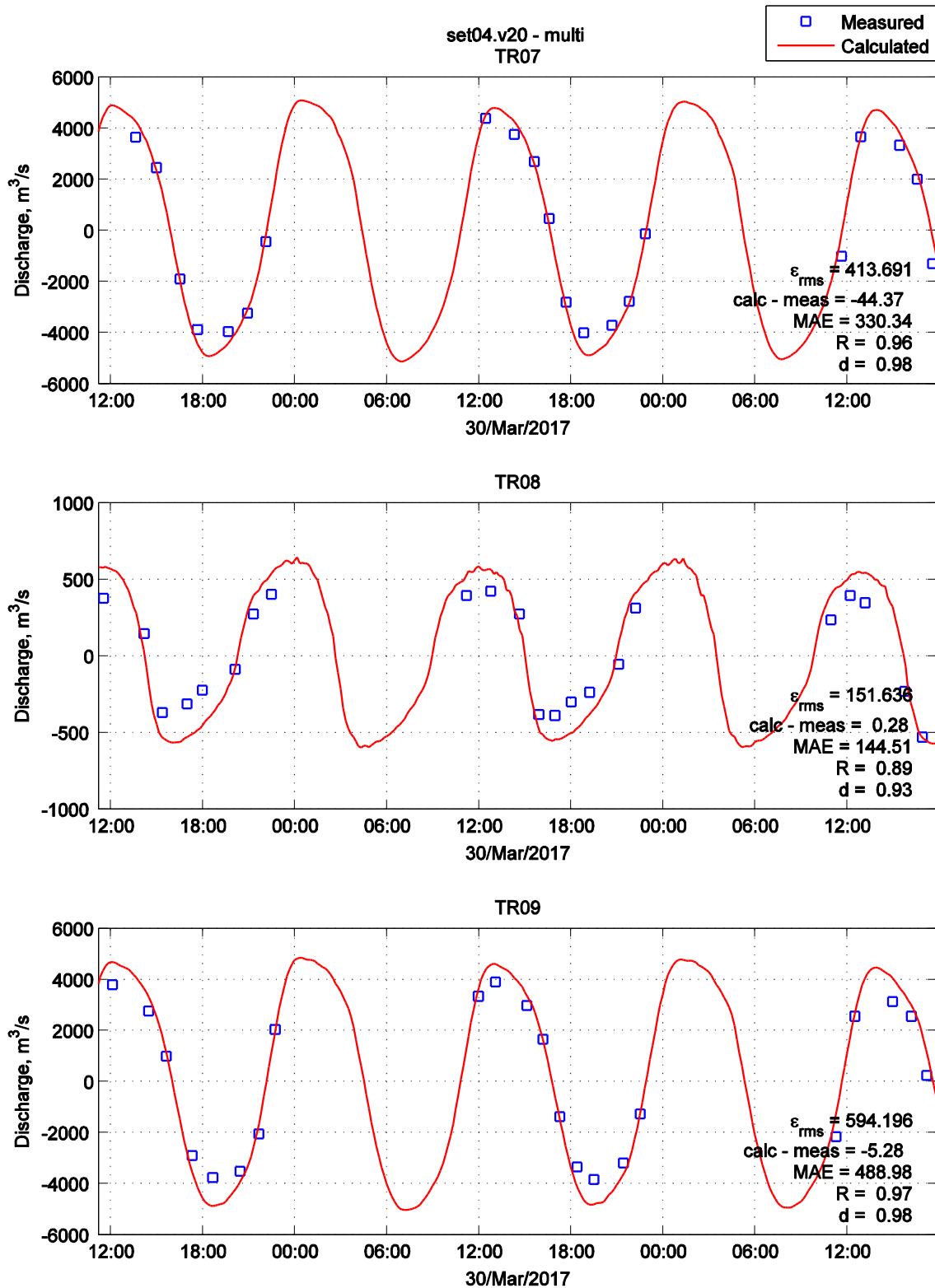
Figure 3-10: Discharge calibration results (TR07 – TR09)
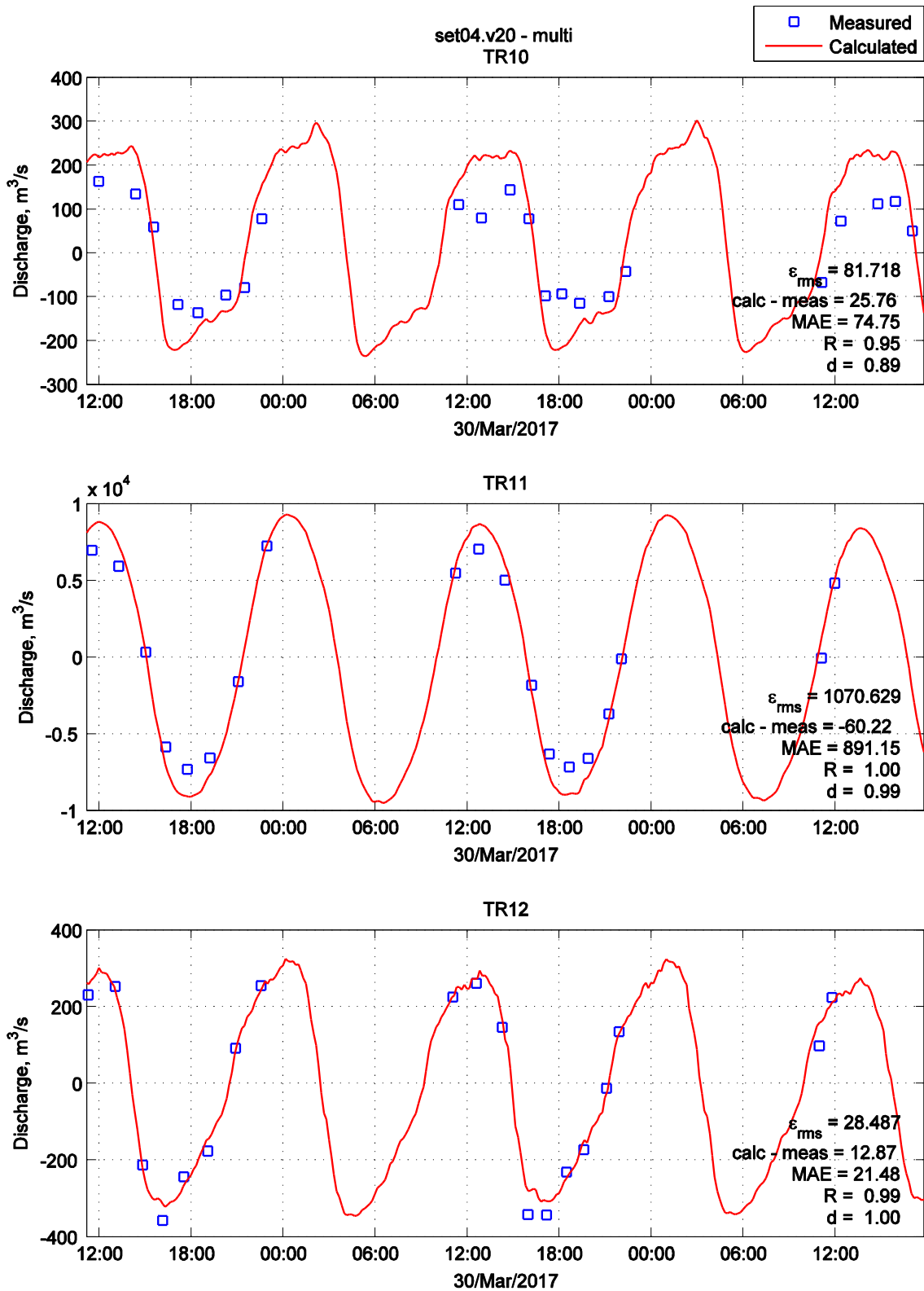
Figure 3-11:   Discharge calibration results (TR10 – TR12)
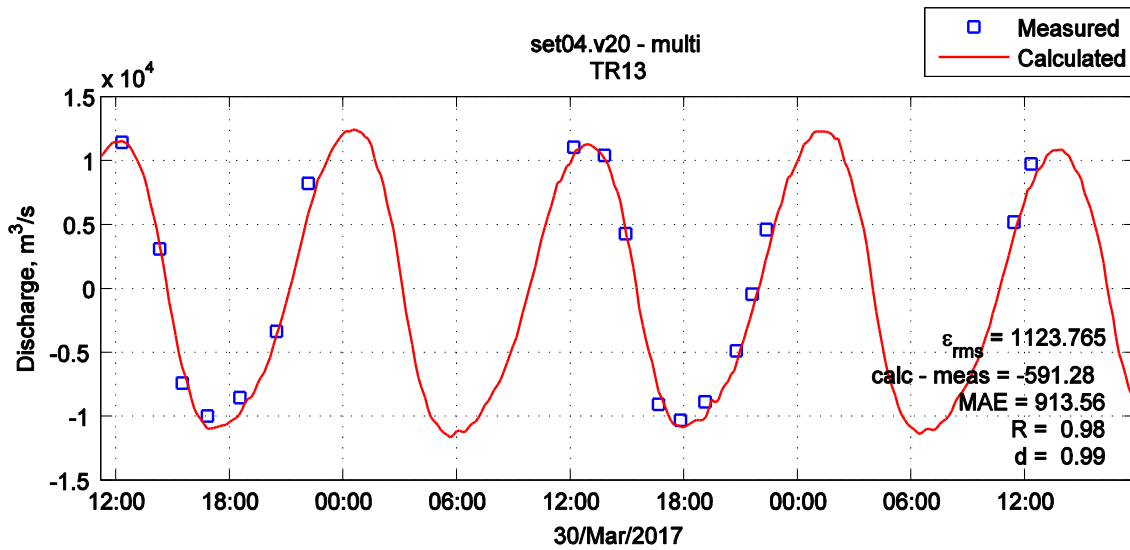
Figure 3-12: Discharge calibration results (TR13)

3.3   FLOW MODEL VALIDATION

For the flow model validation, the water level measurements at NOAA Wilmington Station during Hurricane Matthew in October 2016 were used. The model was forced with time series of measured water levels at Wrightsville Beach (NOAA station 8658163), and wind from the KILM station. It can be seen that the model captures the more extreme water levels well during this hurricane event as shown in Figure 3-13.
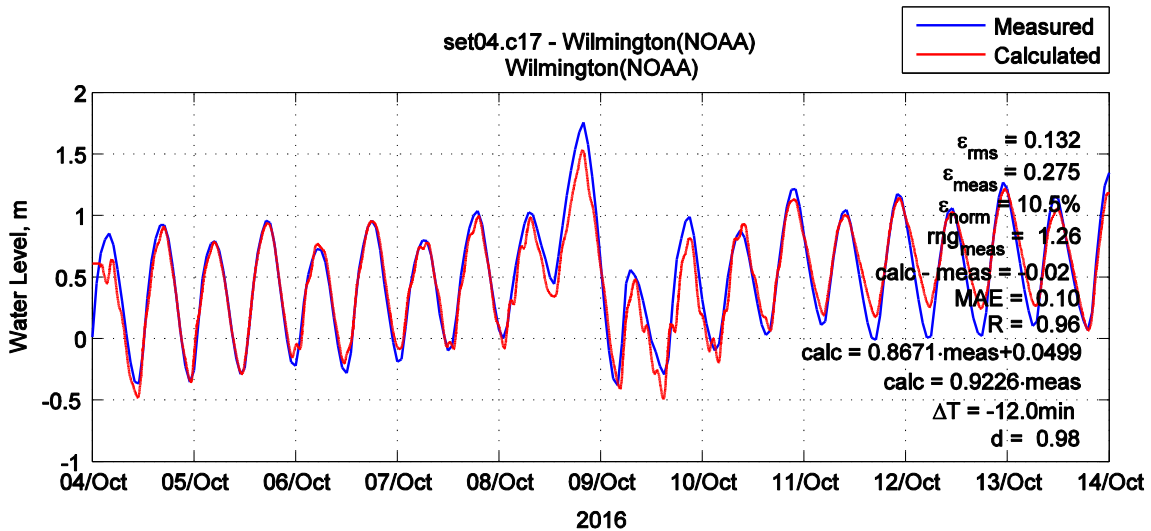
Figure 3-13: Water level validation results during Hurricane Matthew

3.4   WAVE MODEL CALIBRATION

There are six stations (as shown in Figure 2-2) with measured wave data available inside the wave model domains: three NOAA National Data Buoy Center (NDBC) buoys – 41108, Ocean Crest Pier (OCP1), and Sunset Beach Nearshore (SSBN7); three United States Army Corps of Engineers (USACE) Acoustic Doppler Current Profiler (ADCP) gages – Eleven Mile, Bald Head and Oak Island. OCP1 and SSBN7 are owned and maintained by the Coastal Ocean Research and Monitoring Program (CORMP). The NOAA buoy 41108 is at the same location as the USACE Eleven Mile ADCP. The following bulk wave parameters are reported at both the NOAA buoys and the USACE ADCPs: significant wave height, peak and average wave periods, and peak wave direction.

For the wave transformation modeling, in addition to the offshore wave data as the boundary conditions, wind and water level inputs are also important especially during storm events. Based on the contiguous data available at all wave stations along with overlapping wind and water level data, the period of August 1st, 2008 to October 1st, 2008 was selected for the wave model calibration purpose. Large waves generated by Hurricane Hanna were included in this period; thus, the wave model's ability to replicate both large and normal waves can be verified.

3.4.1   Model Inputs

(A)   OFFSHORE WAVE BOUNDARY CONDITIONS

The directional wave spectra from NOAA buoy 41013 were applied as spatially uniform wave conditions at all three boundaries. The wave spectra were calculated based on the spectral wave density, alpha1, alpha2, r1 and r2 data using the extended maximum likelihood method. The description of variables can be found in the NDBC website (www.ndbc.noaa.gov/measdes.shtml), with the conversion method following Earle et al. (1999) and Benoit et al. (1997). Figure 3-14 shows the offshore bulk wave parameters for the calibration period. The maximum wave height of 8.4 m was observed on September 6th, 2008 during Hurricane Hanna.
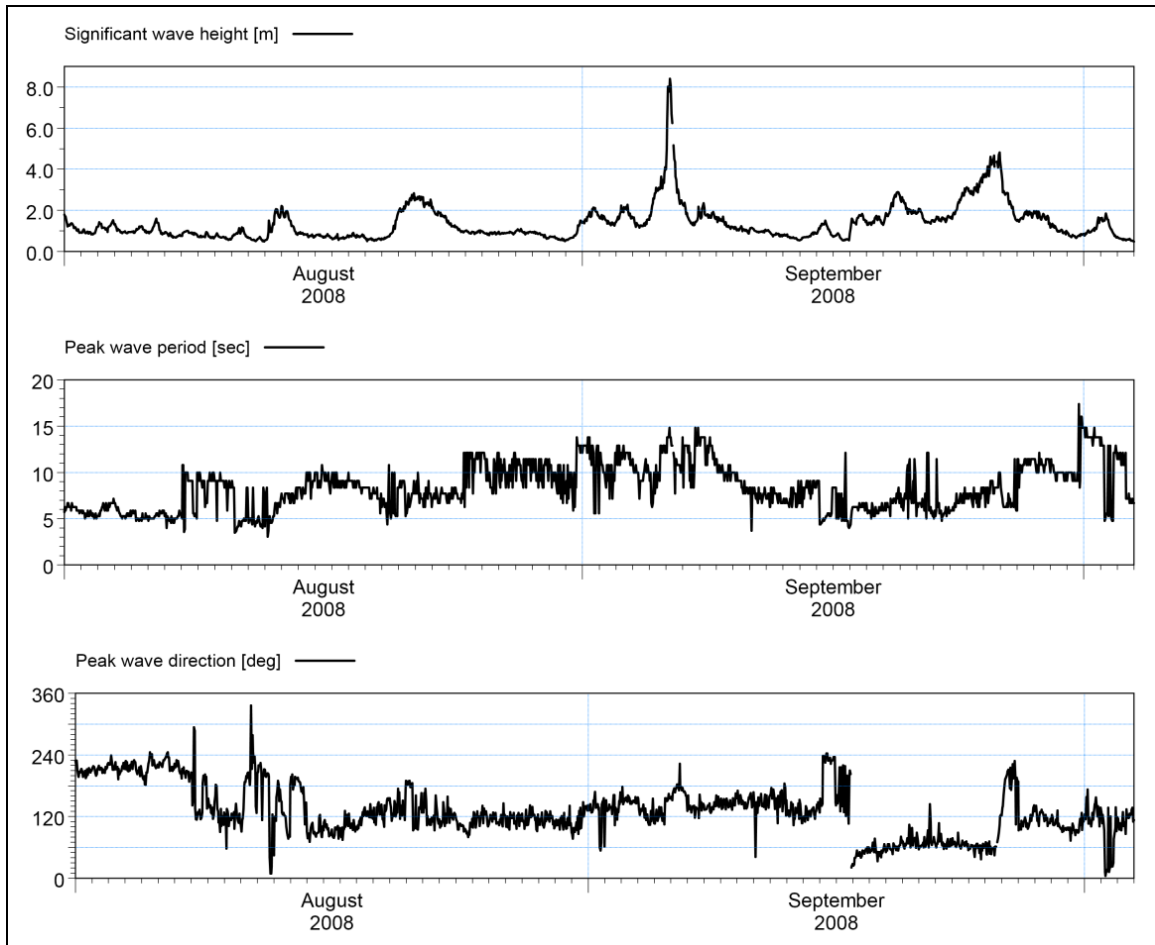
Figure 3-14: Offshore waves from NOAA Buoy 41013 during calibration period

(B)   WINDS

The spatially varying wind data from the National Centers for Environmental Prediction (NCEP) Climate Forecast System Reanalysis (CFSR) were applied for the model calibration period. The CFSR wind data interval is three hours. Figure 3-15 shows wind data comparison between NDBC and CFSR at buoy 41013 with good agreements.
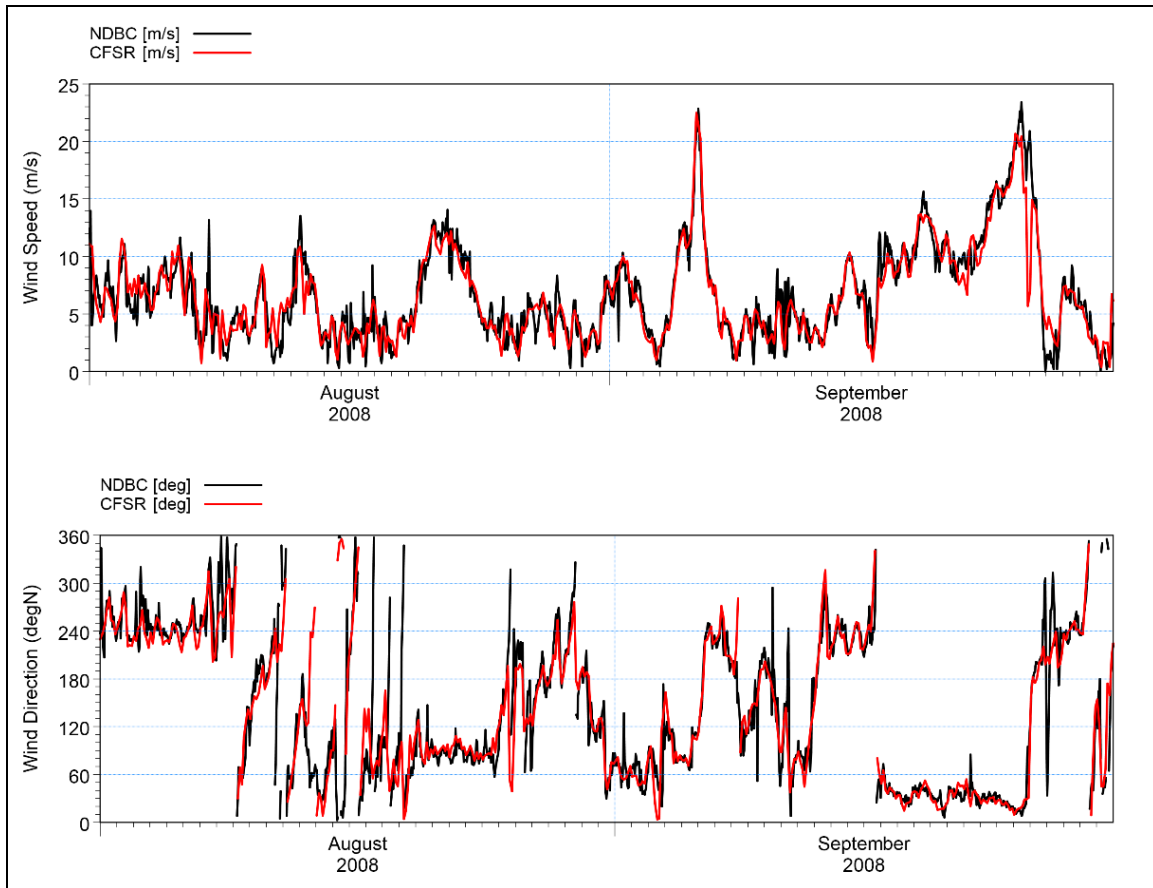
Figure 3-15: Wind data at NOAA buoy 41013 and from CFSR during calibration period

(C)   WATER LEVELS

A spatially uniform water level field was used for the model calibration. Due to the lack of available measured water level data within the model domain, the data from nearby NOAA Station 8658163 at Wrightsville Beach, NC (as shown in Figure 2-1) was used for the model calibration.   Figure 3-16 presents the water level data.   However, it is important to point out that Hurricane Hanna made landfall at the NC/SC border, so the surge was much greater on Oak Island/Bald Head than at Wrightsville Beach.   The reported storm surge was about 5 ft at Wilmington, NC, and about 4 ft at Myrtle Beach, SC, the back side of the storm.   Thus, using the measured water level data at Wrightsville Beach could adversely affect the modeled waves during Hanna. Nonetheless, it's the closest available open coast water level station for the study area and thus used for the wave model calibration without any adjustment.
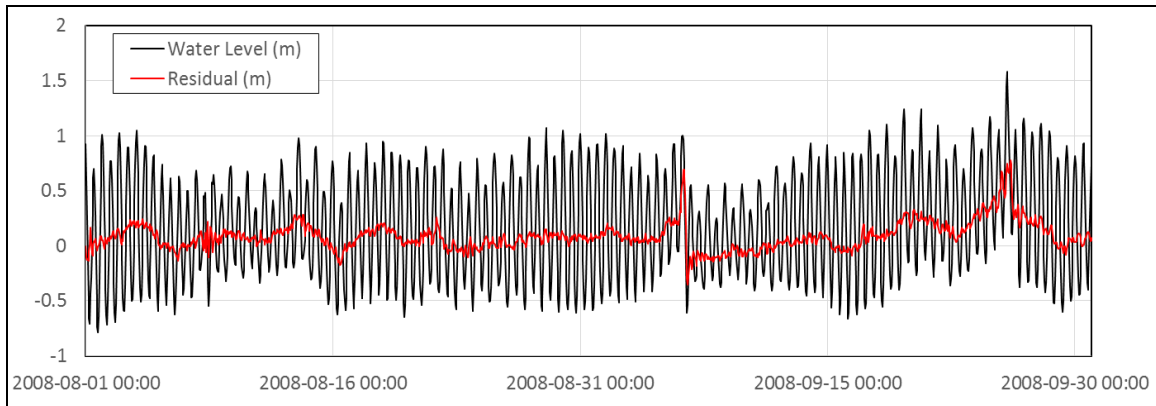
Figure 3-16: Water level data from NOAA station 8658163 for model calibration

3.4.2   Calibration Results

Figure 3-17 through Figure 3-19 present the direct comparison between the computed and measured time series of significant wave height, peak wave period, and peak wave direction, respectively, at the gage locations of Eleven Mile ADCP, Bald Head ADCP, Oak Island ADCP and OCP1. Based on the model bathymetry, the OCP1 ADCP location is at a water depth of 5 m which is close to the wave breaking zone. Because the wave heights during the peak of the storms were greatly under predicted, it is suspected that the depth at the ADCP location was not correct (possibly due to the surge being higher) and therefore the model output point for the OCP1 ADCP was moved offshore to a deeper area of 7 m water depth.
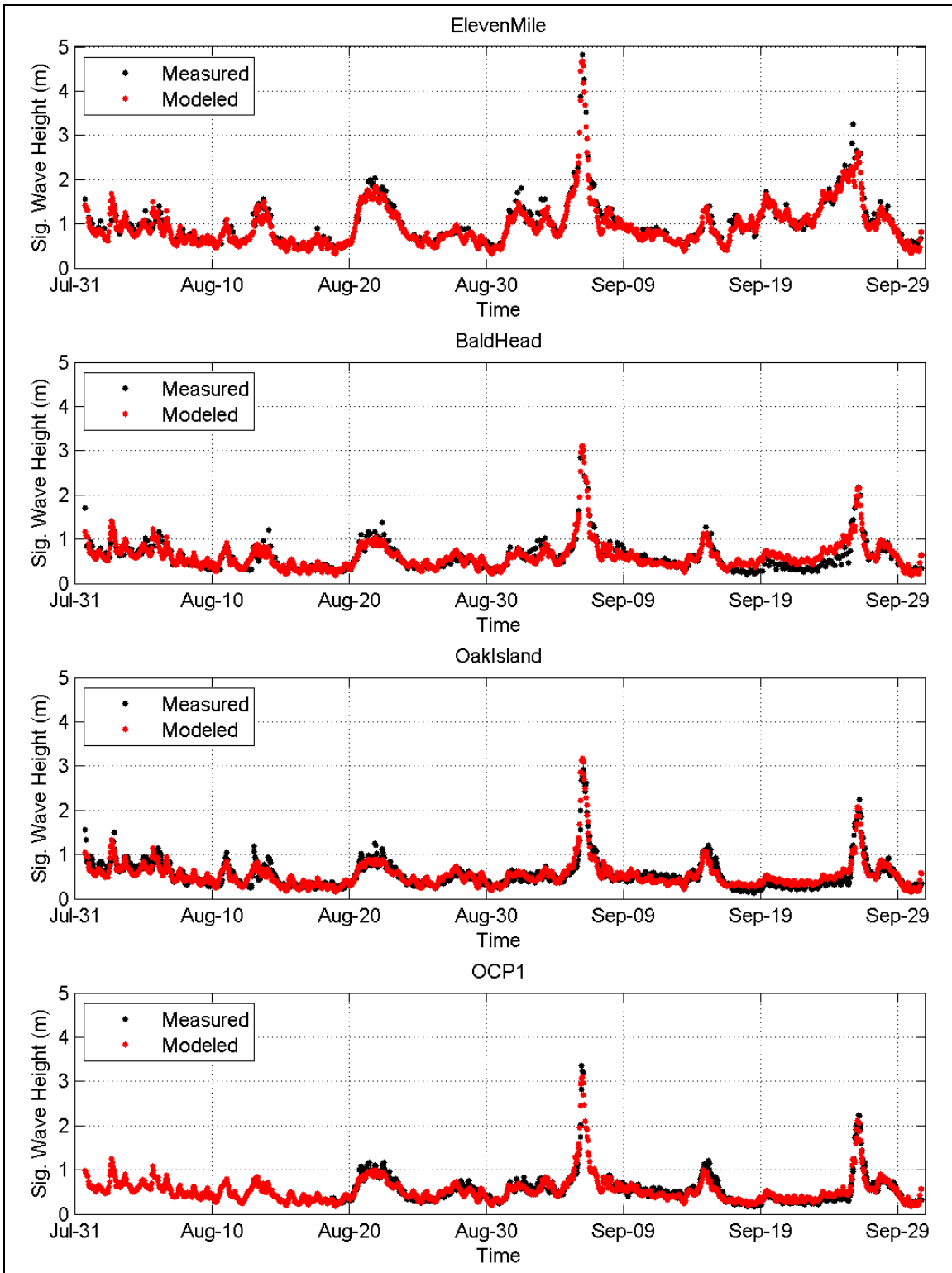
Figure 3-17: Significant wave height calibration results
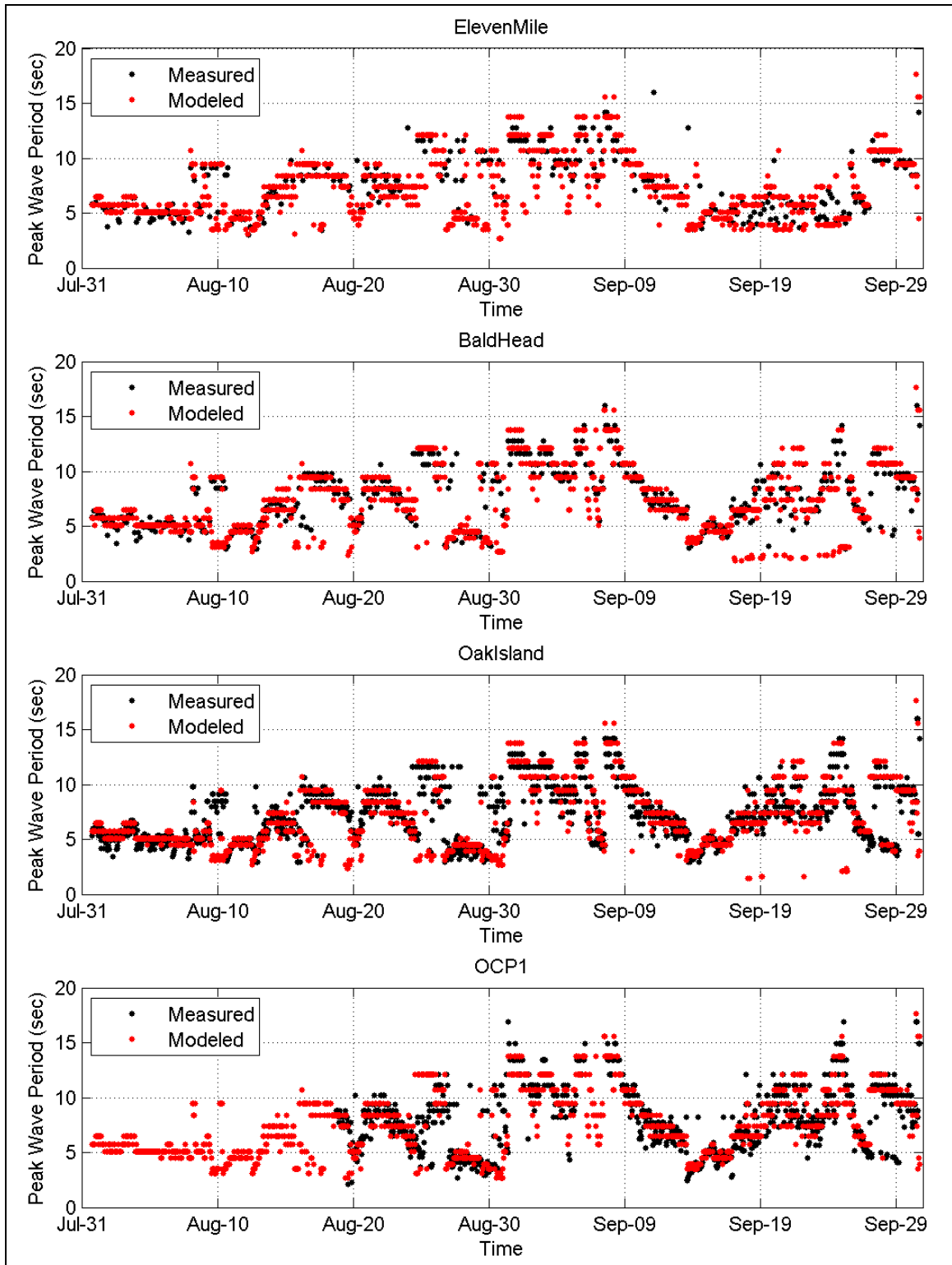
Figure 3-18: Peak wave period calibration results
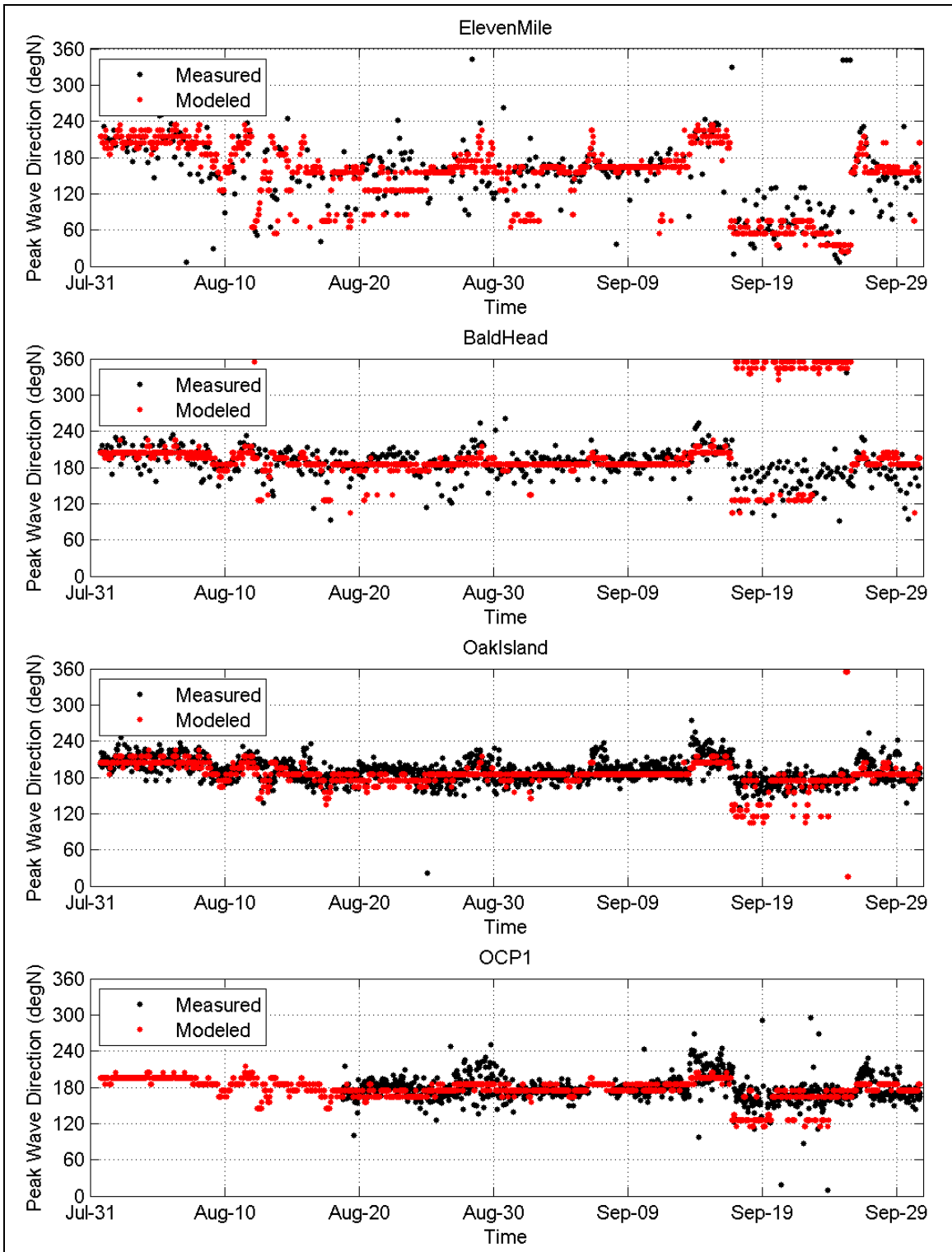
Figure 3-19: Peak wave direction calibration results

The calculated goodness-of-fit parameters for the wave calibration results are listed in Table 3-1 through Table 3-3 for the significant wave height, peak wave period and peak wave direction, respectively. The results suggest that:

- For the significant wave heights, the model predictions agree very well with the measured data at all four ADCP locations, with *MAE* and *RMS* errors less than 0.2 m, and *R* and *d* values greater than 0.9.

- For the peak wave periods, the *MAE* and *RMS* errors are less than 2.5 s, and *R* and *d* values around 0.7 and 0.8, respectively. The data indicates there are periods when at least two wave systems exist – long period waves from offshore and locally generated waves from onshore. In the presence of the two systems, determination of peak period may not be consistent and may alternate between two values. This negatively affects the statistics.

- For the peak wave directions, the model predictions have large deviations from the measured values. It is more pronounced at the Bald Head Island ADCP during period of September 17–26, when the reported ADCP peak wave directions are from between 90 and 180°N, whereas most of the modeled values are from between 330 and 360°N. Figure 3-20 presents both the measured and modeled Bald Head ADCP wave energy spectrum at 1:00 am EST on September 24, 2008. Two wave systems are evident from both the measured and the model predicted spectra: waves coming from SSE–SSW (offshore) with the frequency of around 0.1 Hz; and waves coming from NNW–N (locally wind-generated) with the frequency of around 0.4 Hz. The measured spectrum has some noise at higher frequencies beyond 0.8 Hz. It appears that the peak wave direction from the measured spectrum was calculated to be from offshore; whereas the peak wave direction from the modeled spectrum was calculated to be from onshore. This supports the fact that two or more wave systems can exist at the same time and one can dominate the wave field, which can result in large peak wave direction differences between the measurement and the model prediction. Per communication with USACE personnel[1] who is familiar with the handling of ADCP data, an upper cutoff frequency was used when post-processing the raw ADCP data to the bulk wave parameters. The cutoff frequency was the lesser of the two: when the wavelength is less than two times of the beam separation; or when the pressure response correction for amplitude is 0.1.

---

[1] Personal communication with Kent Hathaway from the USACE.

Table 3-1:   Goodness-of-fit parameters for significant wave height calibration

Station	MAE (m)	RMS (m)	RMSN (%)	R	d
Eleven Mile ADCP	0.14	0.19	4.3	0.96	0.97
Bald Head Island ADCP	0.11	0.15	5.3	0.91	0.95
Oak Island ADCP	0.10	0.13	4.6	0.92	0.96
OCP1 ADCP	0.08	0.11	3.5	0.94	0.97

Table 3-2:   Goodness-of-fit parameters for peak wave period calibration

Station	MAE (s)	RMS (s)	R	d
Eleven Mile ADCP	1.3	2.0	0.74	0.86
Bald Head Island ADCP	1.4	2.4	0.65	0.81
Oak Island ADCP	1.4	2.3	0.64	0.81
OCP1 ADCP	1.4	2.2	0.71	0.85

Table 3-3:   Goodness-of-fit parameters for peak wave direction calibration

Station	MAE (deg)	RMS (deg)
Eleven Mile ADCP	33	46
Bald Head Island ADCP	32	56
Oak Island ADCP	15	23
OCP1 ADCP	15	22
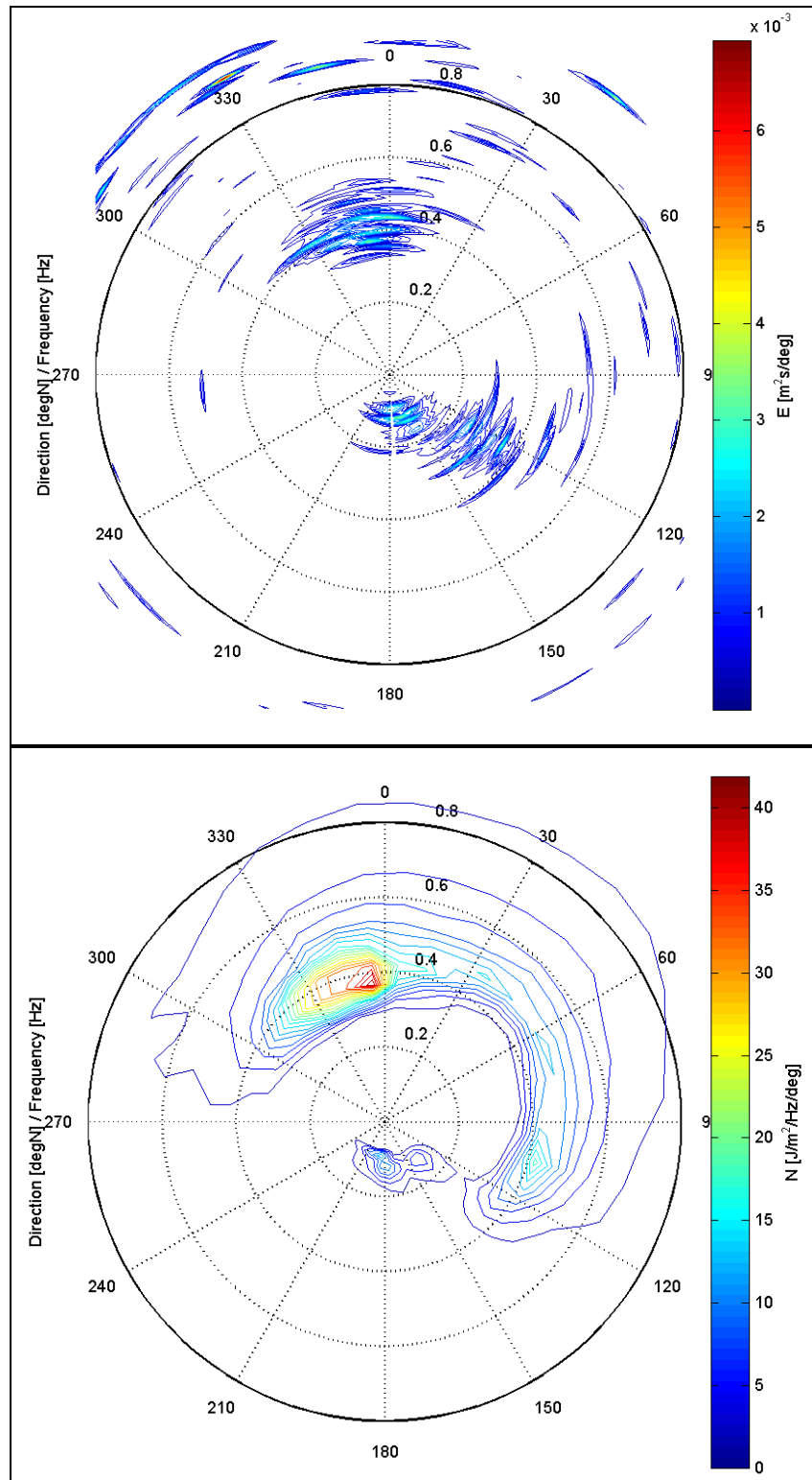
Figure 3-20: Comparison of Bald Head ADCP wave energy spectrum: (up) measured; (down) modeled

3.5 WAVE MODEL VALIDATION

Based on the contiguous data availability at all wave stations along with overlapping wind and water level data, the period of July 1, 2009 to December 1, 2009 was selected for the wave model validation purpose.

Similar to the wave model calibration period, the directional wave spectra from NOAA buoy 41013 were applied as spatially uniform wave conditions; spatially varying wind fields from CFSR were used as the wind inputs; and measured water level data from NOAA station 8658163 were used as a spatially uniform water level field.

Figure 3-21 through Figure 3-23 present the direct comparison between the computed and measured time series of significant wave height, peak wave period and peak wave direction, respectively, at the gage locations of Eleven Mile ADCP, Bald Head ADCP, Oak Island ADCP and OCP1. The goodness-of-fit parameters for the wave validation results are listed in Table 3-4 to Table 3-6 for the significant wave height, peak wave period and peak wave direction, respectively. The results suggest that:

- For the significant wave heights, the model predictions agree very well with the measured data at all four ADCP locations except Oak Island ADCP, with *MAE* and *RMS* errors less than 0.2 m. The wave heights were consistently over-predicted at the Oak Island ADCP. The measured wave heights at Oak Island were lower than OCP1 ADCP; whereas the predicted wave heights were similar. It is possible that the deployment of the Oak Island ADCP during the validation period was in a different depth than previous deployment periods.

- For the peak wave periods, the *MAE* and *RMS* errors are less than 2.6 s, and *R* and *d* values around 0.6 and 0.8, respectively.

- For the peak wave directions, the model predictions have large deviations from the measured values. After checking the measured and model predicted directional wave spectra, the presence of a double peaked spectrum is what caused the issue.
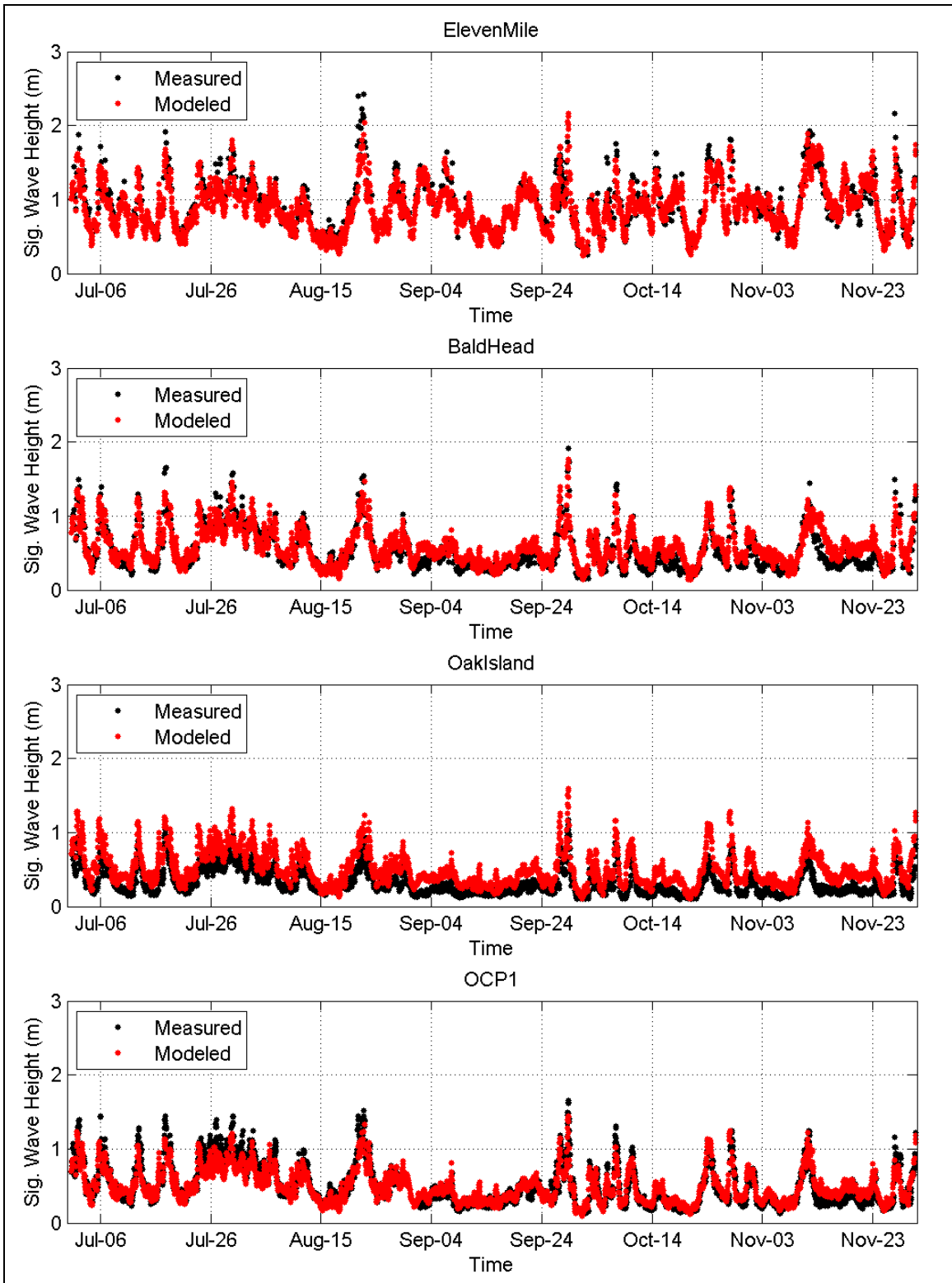
Figure 3-21: Significant wave height validation results
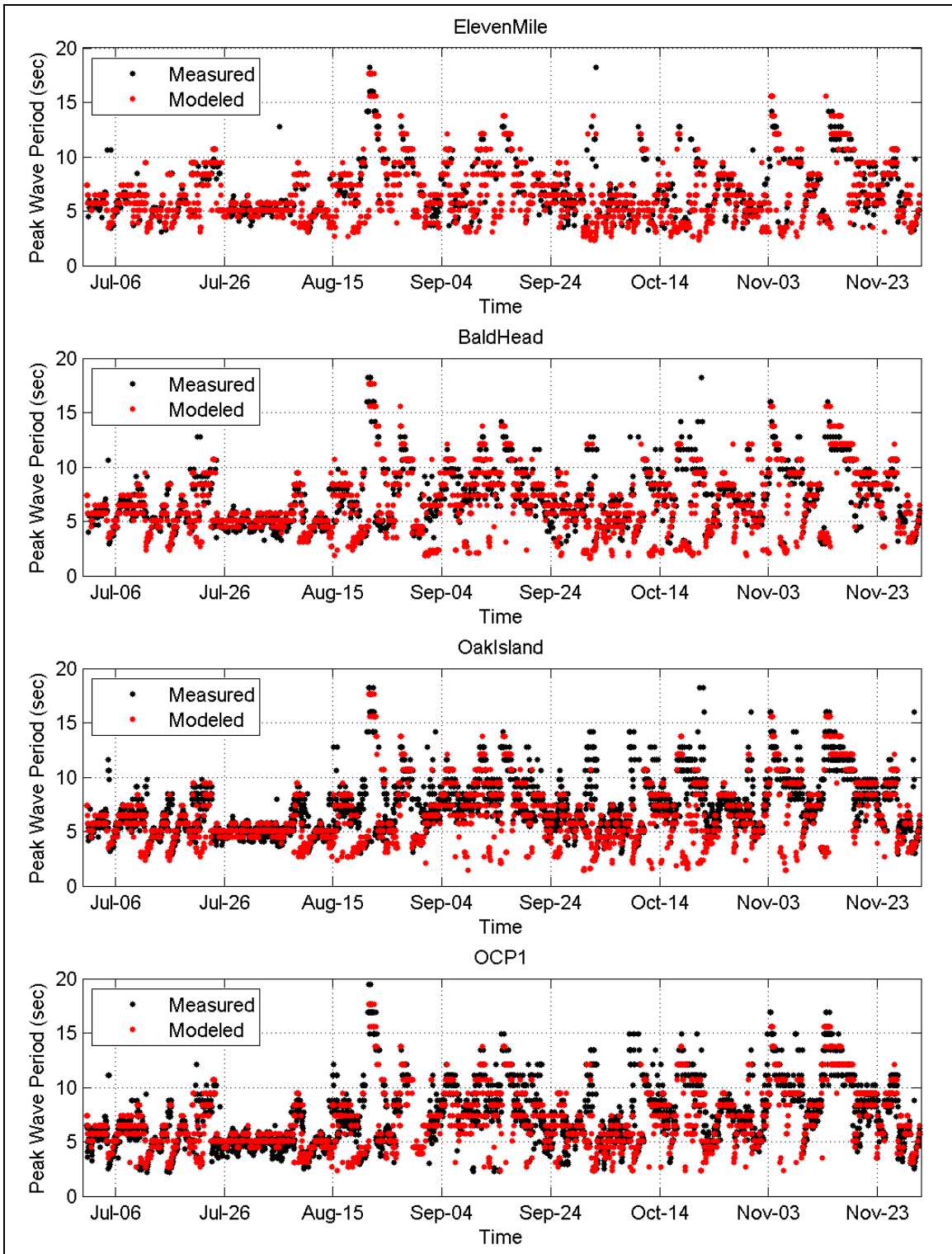
Figure 3-22: Peak wave period validation results
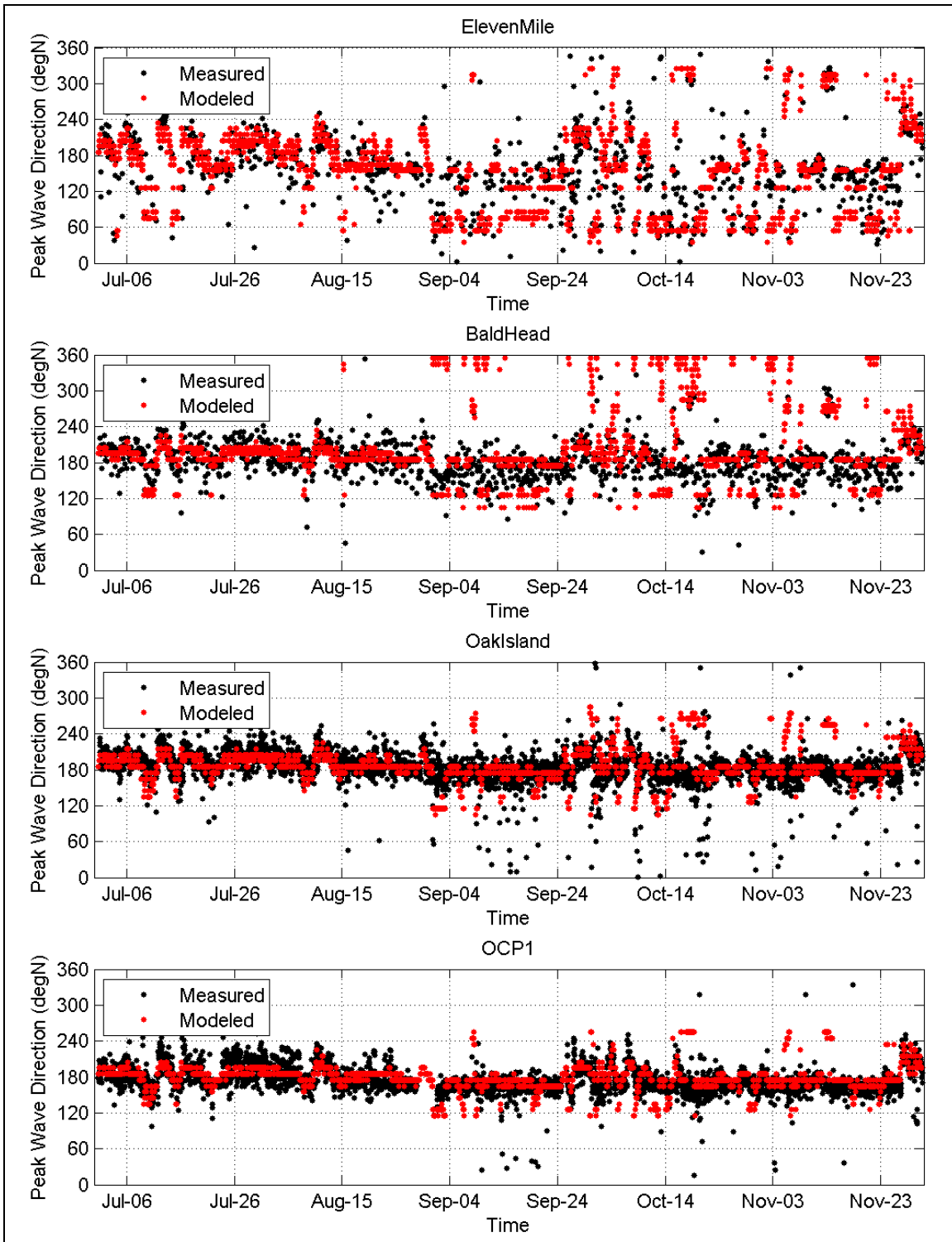
Figure 3-23: Peak wave direction validation results

Table 3-4:   Goodness-of-fit parameters for significant wave height validation

Station	MAE (m)	RMS (m)	RMSN (%)	R	d
Eleven Mile ADCP	0.14	0.18	8.7	0.88	0.93
Bald Head Island ADCP	0.12	0.15	8.6	0.87	0.92
Oak Island ADCP	0.19	0.22	20.3	0.88	0.77
OCP1 ADCP	0.09	0.13	8.2	0.90	0.94

Table 3-5:   Goodness-of-fit parameters for peak wave period validation

Station	MAE (s)	RMS (s)	R	d
Eleven Mile ADCP	1.3	2.1	0.66	0.82
Bald Head Island ADCP	1.5	2.5	0.60	0.78
Oak Island ADCP	1.6	2.6	0.57	0.76
OCP1 ADCP	1.4	2.3	0.68	0.82

Table 3-6:   Goodness-of-fit parameters for peak wave direction validation

Station	MAE (deg)	RMS (deg)
Eleven Mile ADCP	40	56
Bald Head Island ADCP	35	55
Oak Island ADCP	22	35
OCP1 ADCP	18	27

4.   JAY BIRD SHOALS BORROW AREA MODELING

To investigate the potential effects of dredging the identified Jay Bird Shoals borrow area on tidal currents, nearshore waves, and sediment transports along the adjacent shorelines, the existing model bathymetries were modified to reflect the after-dredge conditions.   Two borrow area templates were considered as shown in Figure 4-1. Template 1 includes three zones with dredging elevation down to -26 ft-NAVD88 (Zone 1), -31 ft-NAVD88 (Zone 2), and -27 ft-NAVD88 (Zone 3), respectively. For Template 2, the Zone 2 dredging elevation was reduced to -27 ft-NAVD88 (the same dredging elevation as Zone 3 in Template 1) and its footprint was also reduced. The maximum dredging scenario was considered for both templates, i.e. assuming to remove all the available material identified as beach compatible (2.95 million and 2.34 million cubic yards for Template 1 and 2 respectively). Only part of the available material, 1.1 million cubic yards, will be dredged for the 2019/2020 Renourishment Project.   Figure 4-2 and Figure 4-3 illustrate the after-dredge bathymetries at the Jay Bird Shoals borrow area for Template 1 and 2, respectively.
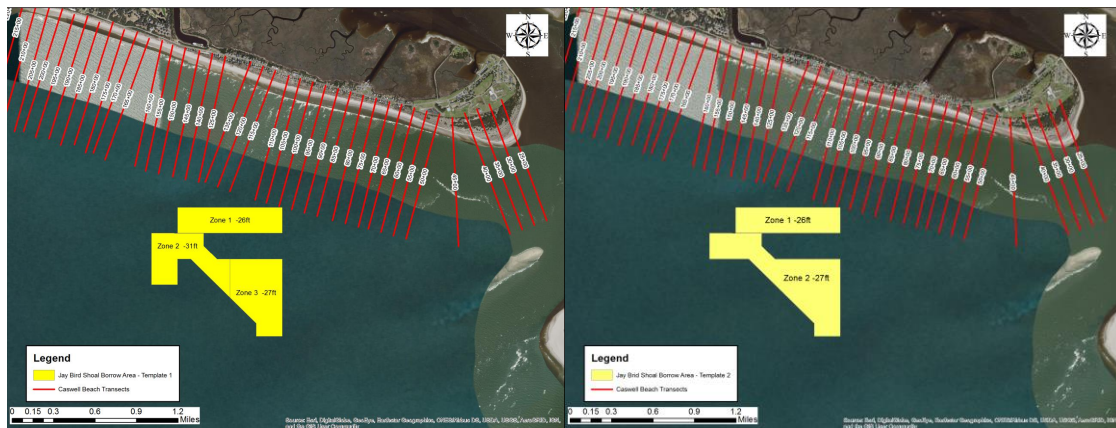
Figure 4-1:   Jay Bird Shoals borrow area templates
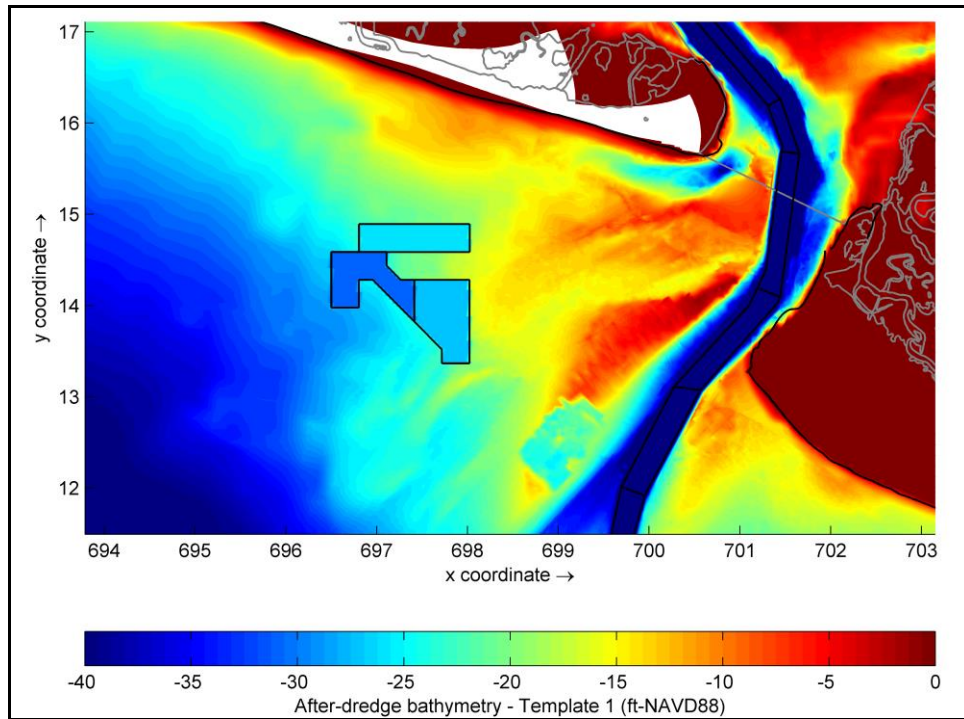
Figure 4-2:   After-dredge bathymetry – Template 1
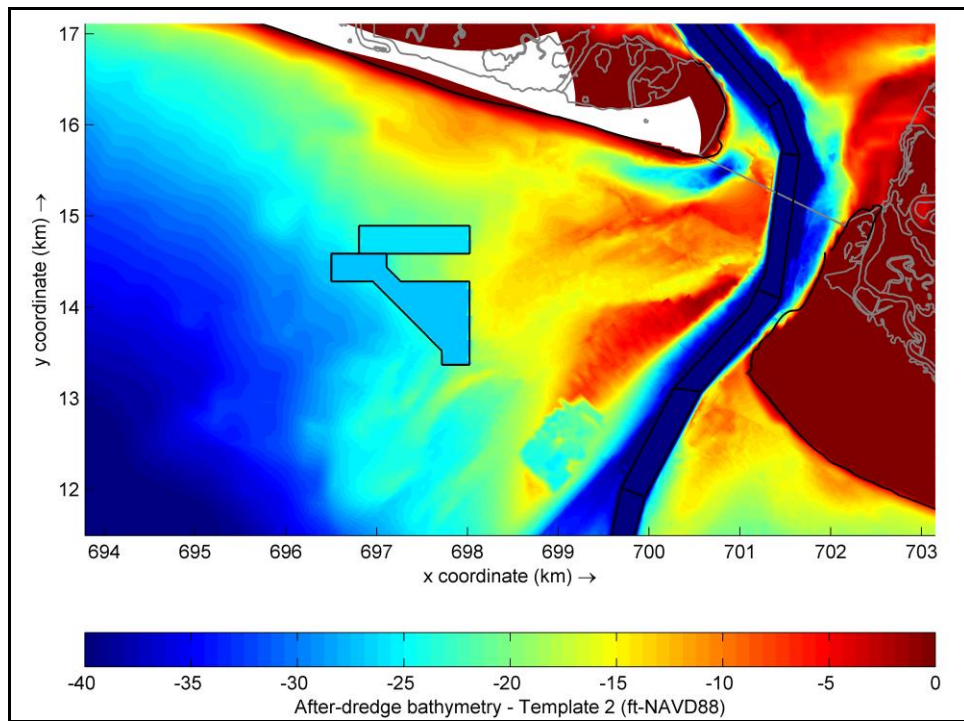
Figure 4-3:   After-dredge bathymetry – Template 2

The modeling results based on the after-dredge bathymetries were compared with the modeling results from the existing bathymetry to identify the potential effects.

4.1   TIDAL CURRENTS

For the existing and the two after-dredge templates, the flow model was simulated for a full spring-neap tidal cycle with astronomical tides and annual average river flows without winds.

4.1.1   Peak Tidal Flood Currents

Figure 4-4, Figure 4-5, and Figure 4-6 present the instantaneous peak flood current velocities during a spring tide under existing and the two after-dredge templates, respectively. Figure 4-7 and Figure 4-8 show the peak flood current velocity differences between the existing and the two after-dredge templates, respectively. The model results indicate that Template 1 would have no measurable changes from existing, Template 2 could cause a 1 ft/s increase of peak flood currents in highly localized areas. Since the project peak current velocity magnitude in these localized areas is less than 1.5 ft/s under all conditions, effects on shorelines are expected to be negligible.
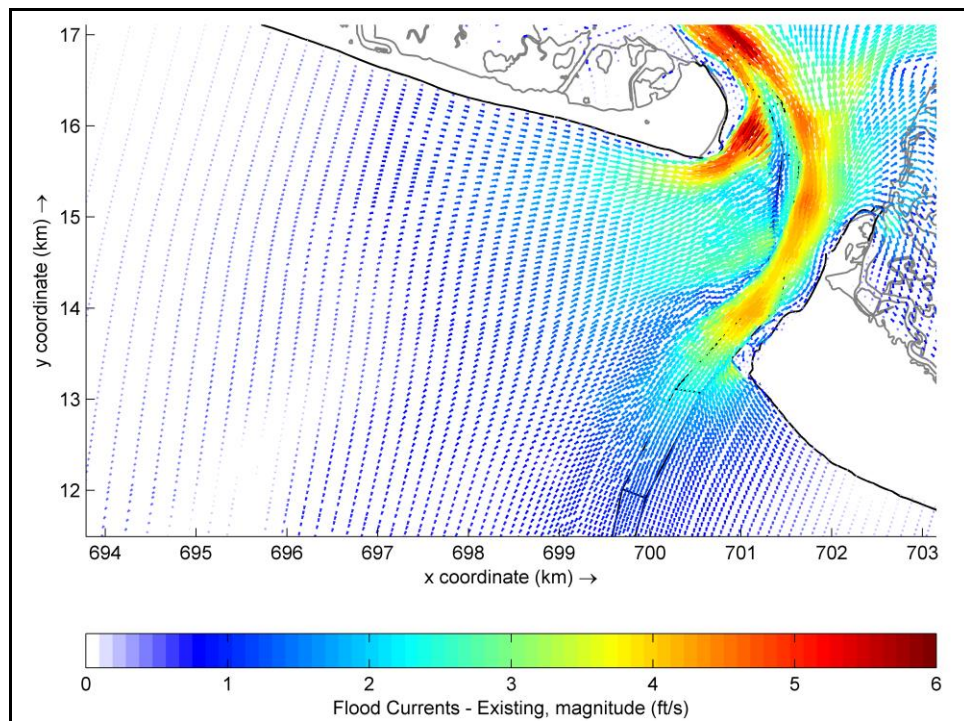
Figure 4-4:   Instantaneous peak flood current velocities – existing condition
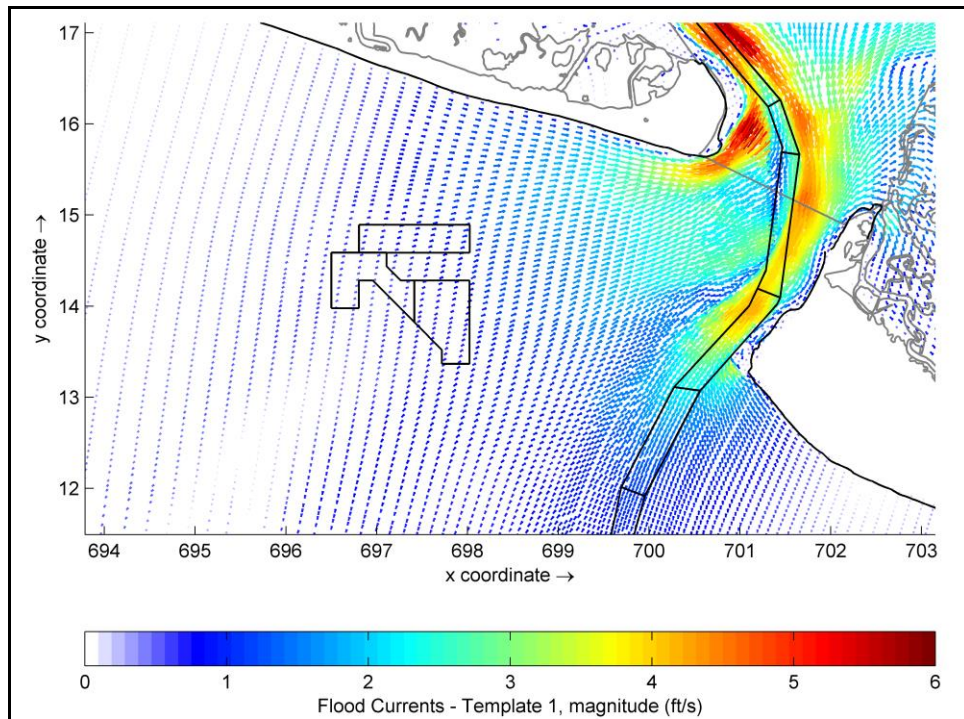
Figure 4-5:   Instantaneous peak flood current velocities – after-dredge Template 1
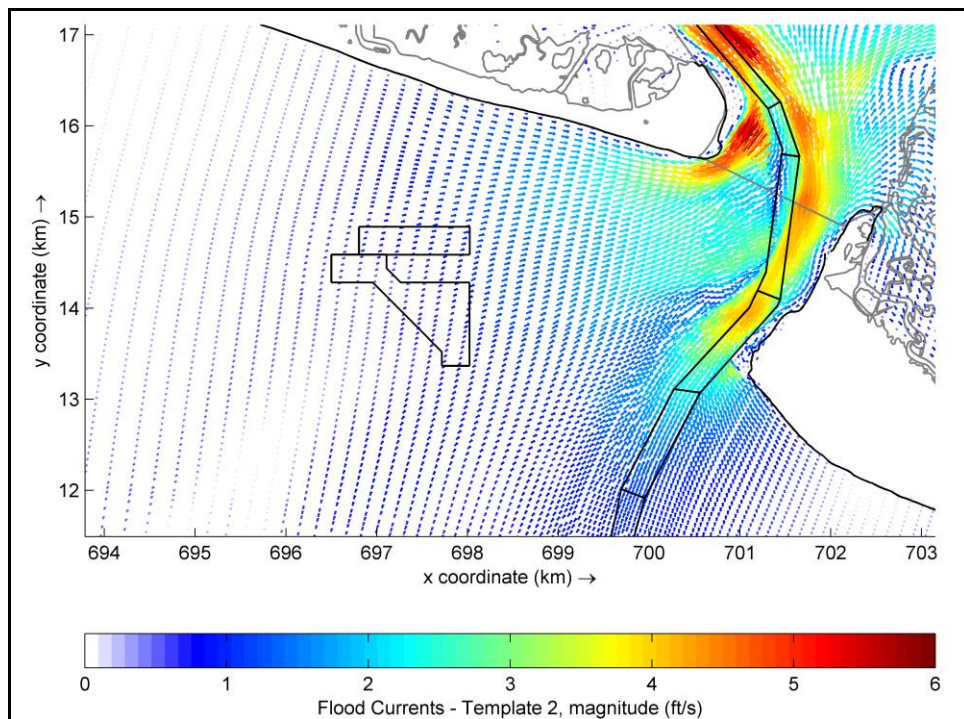
Figure 4-6:   Instantaneous peak flood current velocities – after-dredge Template 2
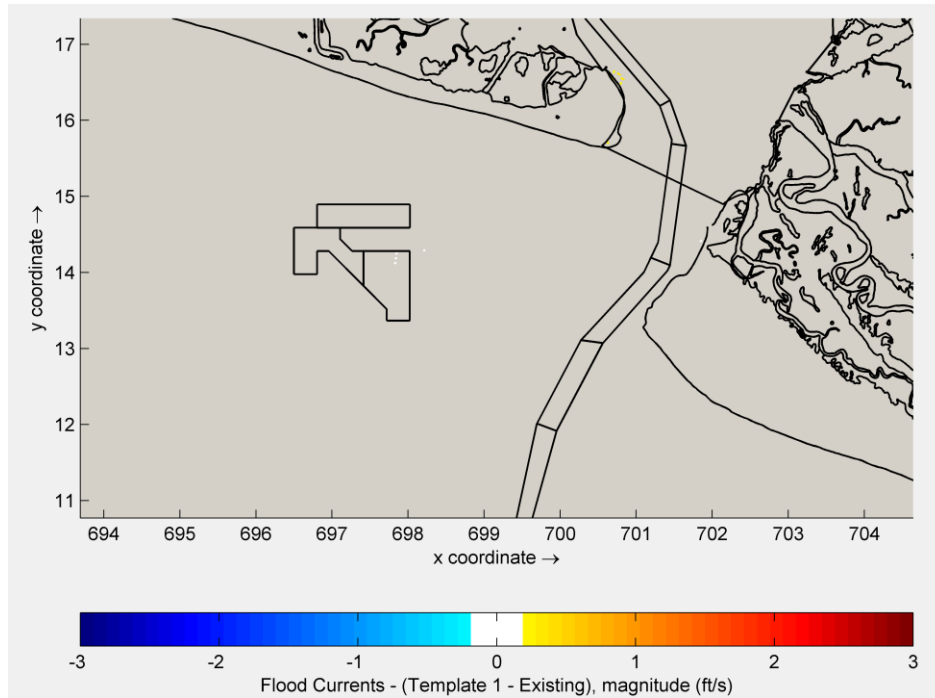
Figure 4-7: After-dredge bathymetry effects on instantaneous peak flood current velocities – Template 1
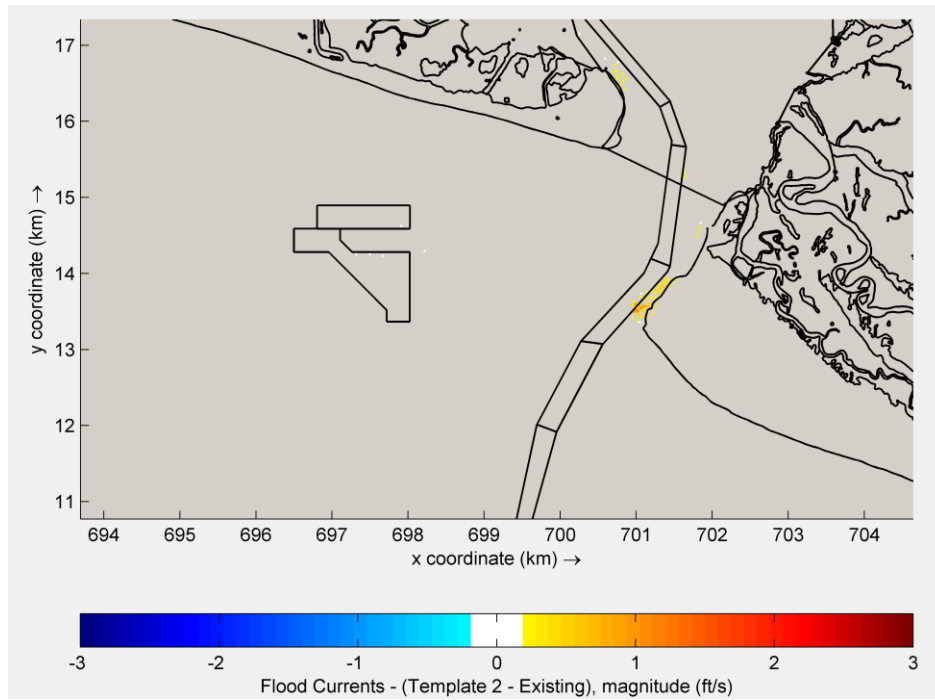
Figure 4-8: After-dredge bathymetry effects on instantaneous peak flood current velocities – Template 2

4.1.2   Residual Tidal Currents

Residual tidal currents over a spring-neap tidal cycle is the "net" flow that remains after subtracting the flood flow vectors from the ebb flow vectors. The residual tidal current pattern is an indicator of potential net movement of sediment over a tidal cycle. In Delft3D, the residual currents are calculated based on Fourier analysis for the current velocities over a specified period.

Figure 4-9 to Figure 4-11 presents the residual tidal currents under the existing and the two after-dredge templates, respectively. The difference of residual tidal currents are shown in Figure 4-12 and Figure 4-13 for Template 1 and 2, respectively. The model results indicate the two after-dredge bathymetry templates could cause negligible residual tidal current increase (less than 0.05 ft/s).
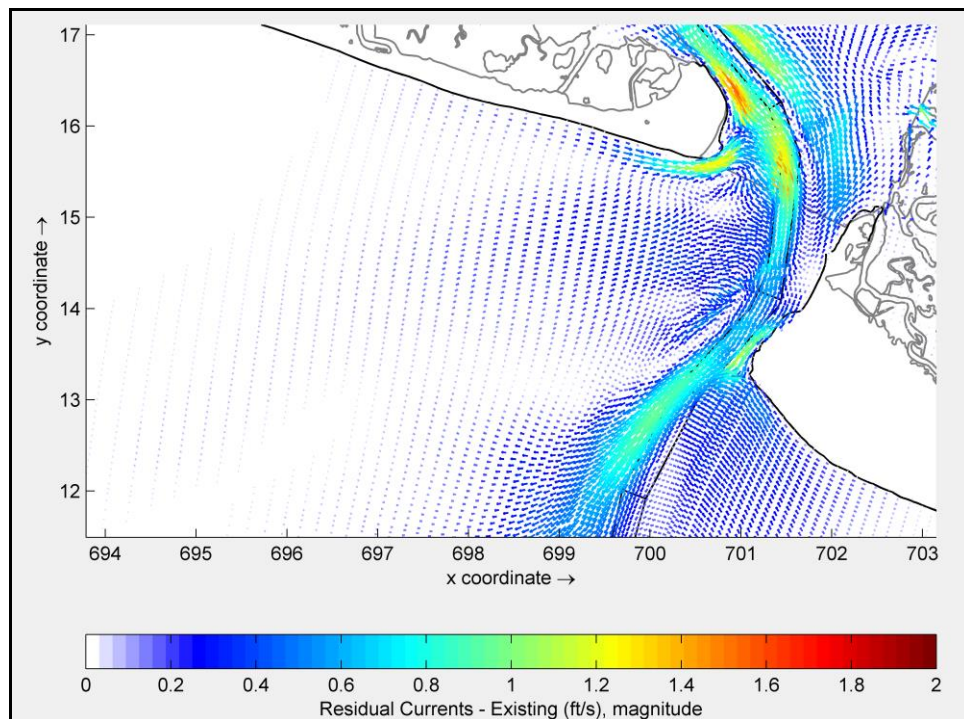
Figure 4-9:   Residual tidal currents – existing condition
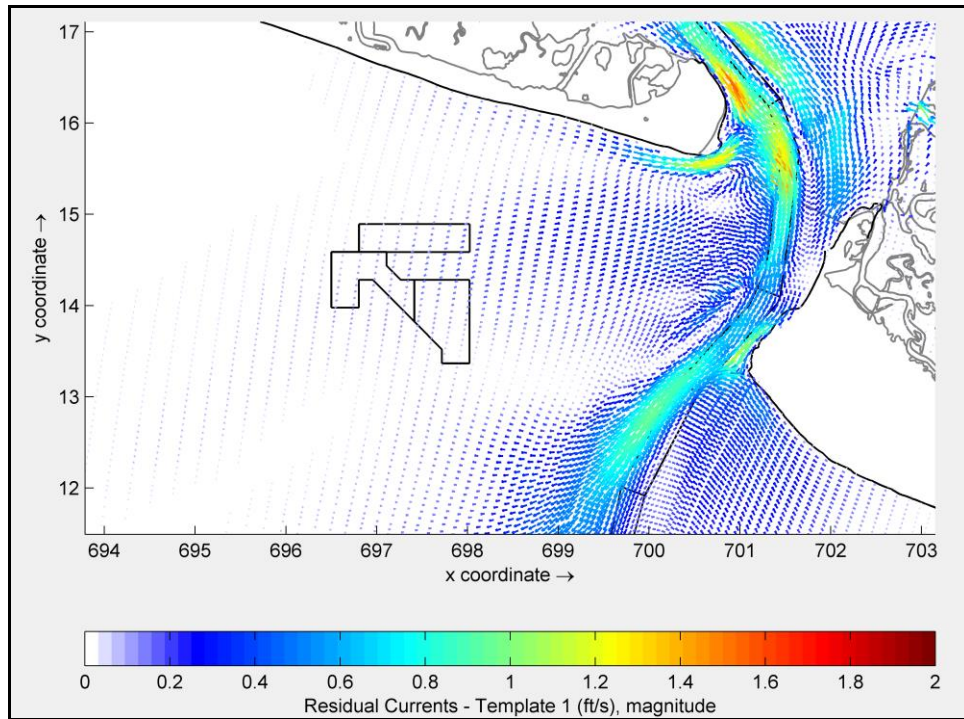
Figure 4-10: Residual tidal currents – after-dredge Template 1
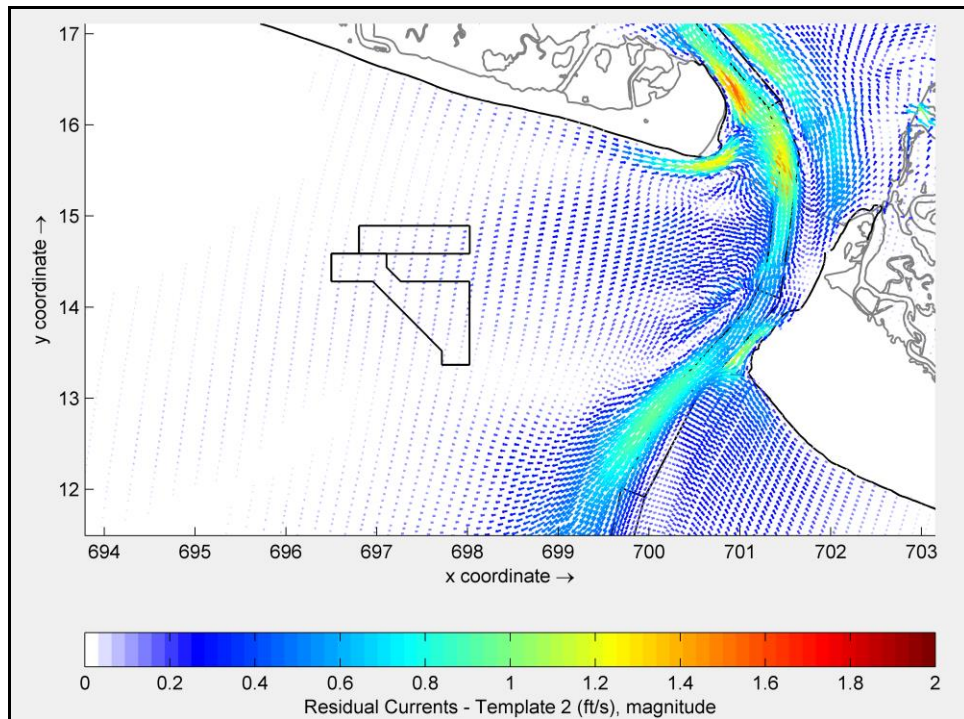
Figure 4-11: Residual tidal currents – after-dredge Template 2
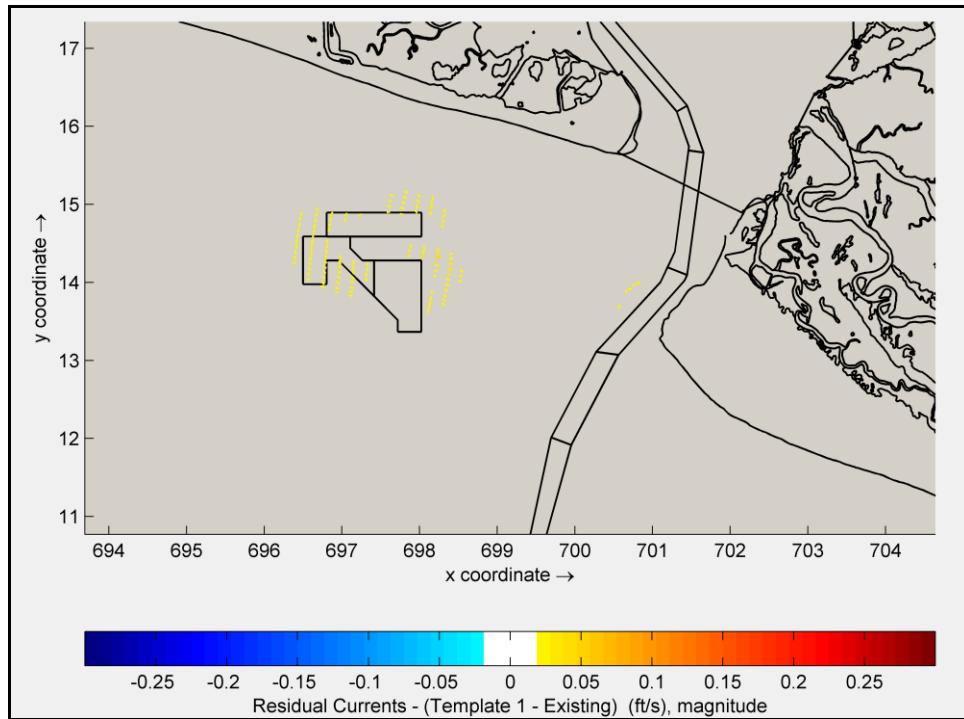
Figure 4-12: After-dredge bathymetry effects on residual tidal currents – Template 1
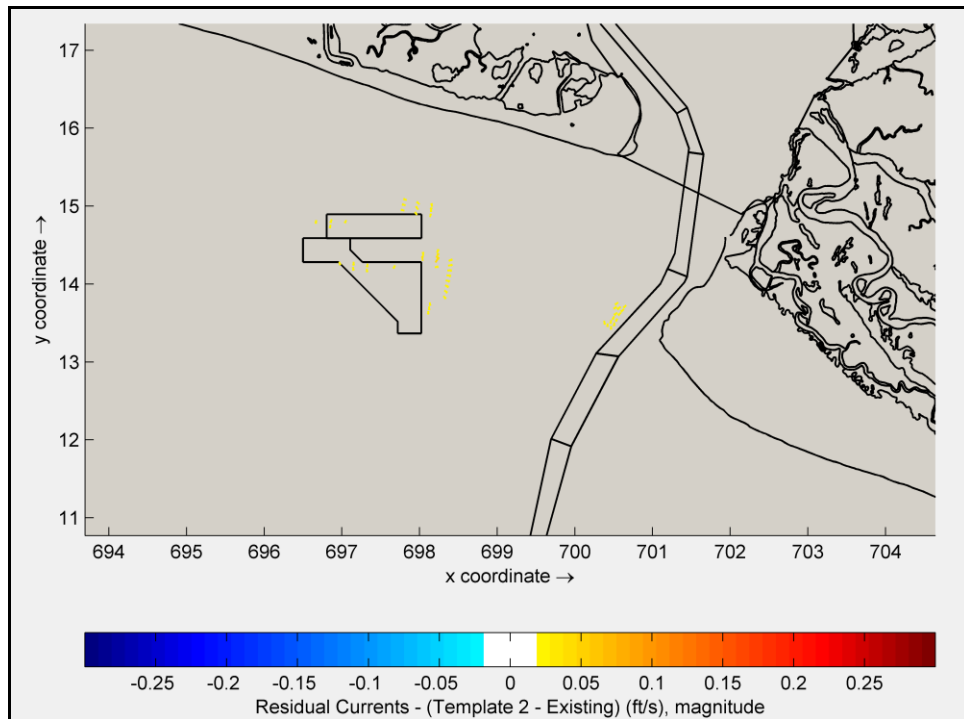
Figure 4-13: After-dredge bathymetry effects on residual tidal currents – Template 2

4.2   WAVES

As stated previously, there were concerns that any potential nearshore wave climate changes caused by the project could affect the adjacent shorelines. For this study, a representative wave approach was adopted to investigate this concern.

4.2.1   Representative offshore waves

The offshore wave data at the NOAA buoy 41013 from 2004 to 2018 was the primary source for deriving the representative input wave conditions. The data gaps in the buoy data were filled with available USACE Wave Information Studies (WIS) hindcast data and NOAA WW3 hindcast data at locations close to 41013. The WIS hindcast data were only available to 2014, so WW3 data were used to fill the data gaps afterwards. The combined wave data were in an hourly time interval. Figure 4-14 shows the annual percentage of exceedance of the significant wave height from the combined offshore wave data. The annual mean significant wave height at the offshore location is about 4.4 ft. Figure 4-15 plots the wave rose for the significant wave height from the combined wave records at offshore. It indicates that the dominant wave direction in the offshore region of the project area is from the ESE. Wave heights less than 6 ft comprise about 80% of the 15-year record.
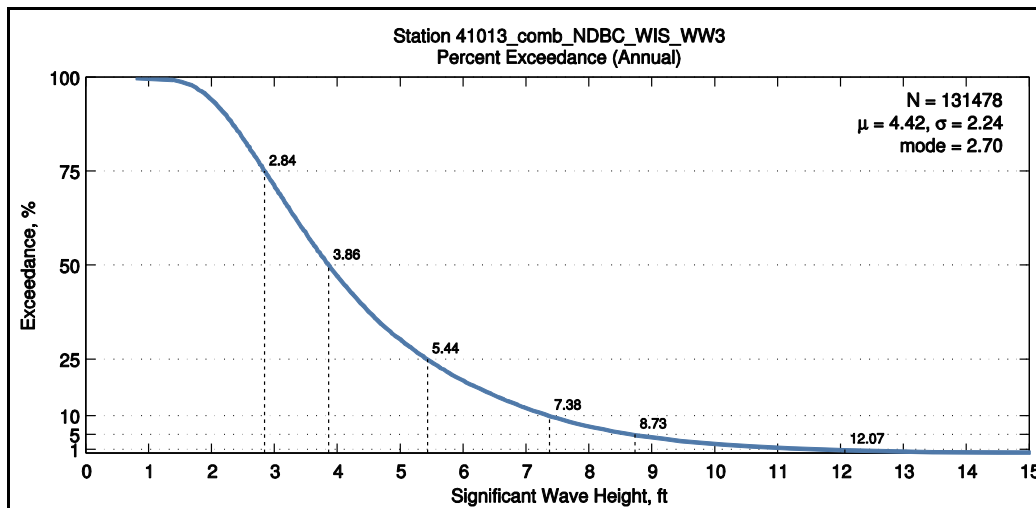
Figure 4-14: Annual percentage of exceedance of significant wave height at the offshore boundary

Significant Wave Height (Annual)
Station 41013_comb_NDBC_WIS_WW3
Period 01-Jan-2004 to 31-Dec-2018

Direction FROM is shown
Center value indicates calms below 0 ft
Total observations 131478, calms 0
About 0.0144% of observations missing

Percentage of Occurrence

Significant Wave Height, ft	N	NNE	NE	ENE	E	ESE	SE	SSE	S	SSW	SW	WSW	W	WNW	NW	NNW	Total
Total	0.60	1.77	4.31	9.39	12.76	17.84	14.62	9.15	9.75	8.62	6.16	1.66	0.99	0.95	0.72	0.72	100.00
15																	0.23
12				0.10	0.11	0.11	0.12		0.13								0.80
9			0.15	0.55	0.33	0.22	0.34	0.37	0.49	0.37	0.24	0.12					3.34
6		0.36	1.14	2.56	1.20	1.45	1.34	1.44	1.88	1.32	1.05	0.33	0.30	0.24	0.18	0.19	15.07
3	0.42	1.17	2.57	4.53	5.91	8.30	7.23	4.55	5.33	5.10	3.74	0.85	0.47	0.52	0.42	0.43	51.53
0		0.22	0.44	1.64	5.17	7.73	5.56	2.67	1.89	1.74	1.10	0.36	0.16	0.14			29.03

ft
≥ 15
12 – 15
9 – 12
6 – 9
3 – 6
0 – 3

Figure 4-15: Wave rose of significant wave heights at the offshore boundary

In order to derive representative wave conditions, the 15-year wave record was sorted by peak wave direction and significant wave height. The sorting routine contained 24 direction bins (15 degrees each) and nine significant wave height bins (1 m each). Only waves which would reasonably be expected to affect the project shorelines were considered specifically including waves originating from between East (90 degrees) and West (270 degrees) azimuth. This resulted in 86 wave cases used as model input and which represent approximately 75.4% of the 15-year record by occurrence (waves from east to north to west were excluded). The average wave parameters were calculated in each wave case. Table 4-1 lists the characteristics of each wave case as they were applied to the wave modeling.

Table 4-1:   Representative wave conditions used as model inputs

Hs_bin (m)	MWD_bin (degN)	Bin average sig. wave height (ft)	Bin average peak wave period (s)	Bin average Wave Direction (degN)	Percentage Occurrence
0 - 1	90 - 105	2.5	9.0	97.7	4.854
1 - 2	90 - 105	4.4	9.5	98.0	3.973
2 - 3	90 - 105	7.8	10.1	97.3	0.635
3 - 4	90 - 105	11.3	11.8	97.1	0.164
4 - 5	90 - 105	14.2	12.4	98.0	0.054
5 - 6	90 - 105	17.5	13.9	99.0	0.016
6 - 7	90 - 105	20.7	13.1	98.0	0.002
0 - 1	105 - 120	2.4	8.9	112.5	6.297
1 - 2	105 - 120	4.4	9.4	112.4	5.030
2 - 3	105 - 120	7.7	9.6	112.8	0.714
3 - 4	105 - 120	11.3	10.9	112.2	0.129
4 - 5	105 - 120	14.1	12.2	112.0	0.038
5 - 6	105 - 120	17.6	11.2	115.9	0.005
6 - 7	105 - 120	20.7	12.3	115.8	0.002
7 - 8	105 - 120	23.3	15.3	115.1	0.002
0 - 1	120 - 135	2.5	8.6	126.9	5.573
1 - 2	120 - 135	4.4	9.0	127.3	4.728
2 - 3	120 - 135	7.7	9.6	127.1	0.789
3 - 4	120 - 135	11.1	10.1	128.1	0.135
4 - 5	120 - 135	14.4	10.2	126.9	0.035
5 - 6	120 - 135	18.0	11.3	128.7	0.010

6 - 7	120 - 135	20.2	12.2	130.1	0.002
8 - 9	120 - 135	26.8	14.8	128.6	0.002
0 - 1	135 - 150	2.5	8.0	141.6	3.391
1 - 2	135 - 150	4.5	8.3	142.0	3.696
2 - 3	135 - 150	7.8	8.9	142.5	0.646
3 - 4	135 - 150	11.3	9.9	142.2	0.193
4 - 5	135 - 150	14.1	10.4	142.1	0.054
5 - 6	135 - 150	18.3	11.1	142.9	0.011
6 - 7	135 - 150	20.2	12.3	142.6	0.003
7 - 8	135 - 150	25.2	15.9	141.2	0.002
8 - 9	135 - 150	27.6	14.8	143.3	0.001
0 - 1	150 - 165	2.6	7.1	156.9	2.225
1 - 2	150 - 165	4.6	7.4	157.3	2.810
2 - 3	150 - 165	7.8	8.1	157.7	0.739
3 - 4	150 - 165	11.0	9.2	157.3	0.174
4 - 5	150 - 165	14.6	9.7	157.6	0.035
5 - 6	150 - 165	17.4	11.1	154.1	0.007
6 - 7	150 - 165	20.5	11.9	154.8	0.003
7 - 8	150 - 165	23.9	13.0	159.0	0.001
0 - 1	165 - 180	2.7	6.1	172.3	1.770
1 - 2	165 - 180	4.6	6.7	172.6	3.194
2 - 3	165 - 180	7.8	8.0	172.5	1.012
3 - 4	165 - 180	11.1	9.0	172.9	0.204
4 - 5	165 - 180	14.3	9.6	173.7	0.029
5 - 6	165 - 180	17.6	11.2	169.7	0.004
6 - 7	165 - 180	20.7	12.0	175.7	0.004
7 - 8	165 - 180	25.8	13.8	169.7	0.002
8 - 9	165 - 180	26.8	14.2	170.8	0.002
0 - 1	180 - 195	2.7	5.5	187.0	1.607
1 - 2	180 - 195	4.5	6.4	187.2	3.474
2 - 3	180 - 195	7.9	8.0	186.7	1.063
3 - 4	180 - 195	11.2	9.2	186.9	0.232
4 - 5	180 - 195	14.2	10.0	186.9	0.050
5 - 6	180 - 195	17.6	11.2	186.6	0.005

6 - 7	180 - 195	20.2	12.8	183.0	0.001
0 - 1	195 - 210	2.7	5.1	202.1	1.613
1 - 2	195 - 210	4.5	6.0	202.4	3.239
2 - 3	195 - 210	7.8	7.6	201.7	0.727
3 - 4	195 - 210	11.1	8.9	201.9	0.189
4 - 5	195 - 210	14.3	9.4	201.9	0.040
5 - 6	195 - 210	17.0	10.0	199.6	0.003
0 - 1	210 - 225	2.7	4.9	216.8	1.319
1 - 2	210 - 225	4.6	5.8	217.1	3.141
2 - 3	210 - 225	7.7	7.2	217.4	0.666
3 - 4	210 - 225	11.0	8.3	217.9	0.115
4 - 5	210 - 225	14.2	9.2	215.3	0.015
5 - 6	210 - 225	16.8	8.3	219.7	0.001
0 - 1	225 - 240	2.6	4.6	231.3	0.688
1 - 2	225 - 240	4.6	5.5	230.8	1.609
2 - 3	225 - 240	7.8	7.0	231.2	0.367
3 - 4	225 - 240	10.8	8.3	231.0	0.071
4 - 5	225 - 240	14.2	9.2	228.9	0.007
5 - 6	225 - 240	17.4	8.8	231.2	0.005
0 - 1	240 - 255	2.6	4.9	246.5	0.301
1 - 2	240 - 255	4.7	5.5	246.3	0.539
2 - 3	240 - 255	7.9	6.7	246.4	0.190
3 - 4	240 - 255	10.8	7.4	246.9	0.039
4 - 5	240 - 255	13.5	7.5	249.3	0.002
5 - 6	240 - 255	17.8	8.6	248.0	0.001
0 - 1	255 - 270	2.6	4.8	261.3	0.169
1 - 2	255 - 270	4.7	5.4	262.0	0.321
2 - 3	255 - 270	7.8	6.3	262.3	0.168
3 - 4	255 - 270	10.7	6.9	261.3	0.040
4 - 5	255 - 270	15.0	8.2	259.0	0.002
5 - 6	255 - 270	17.9	8.3	263.5	0.002

4.2.2   Nearshore Wave Results

Each of the 86 wave conditions listed in Table 4-1 were run for the existing bathymetric condition and of the two after-dredge bathymetry templates. Winds and water levels were not included in these model runs. For each discrete wave condition, the spatial map of significant wave height (after-dredge Hs – existing Hs) was calculated. It is expected and confirmed by the model results that nearshore waves would decrease leeward of the Jay Bird Shoals borrow area due to wave refraction caused by the excavated borrow area. At the same time nearshore waves could increase slightly on both the east and west side of the borrow area. Some results from the 86 wave conditions are presented below, all wave condition model results are included in Appendix C1 and C2 for Template 1 and Template 2, respectively.

Figure 4-16 presents the model results for representative waves in the range of 0 – 3 ft originating from Southeast (SE), South (S), and Southwest (SW). The waves in this range comprise about 30% of the 15-year record. The average wave height is about 2.5 ft. The two after-dredge bathymetry templates show that effects from these small wave conditions are negligible. Vectors represent the modeled wave directions from the two after-dredge bathymetry templates.

Figure 4-17 presents the model results for representative waves in the range of 3 – 6 ft originating from SE, S, and SW. The waves in this range comprise about 50% of the 15-year record. The average significant wave height is about 4.5 ft which is approximately the annual average wave conditions in the offshore area. The two after-dredge bathymetry templates could cause about 3 inches of wave height increase in highly localized areas offshore of the shoreline.

Figure 4-18 shows the model results for representative waves in the range of 6 – 9 ft originating from SE, S, and SW. The waves in this range comprise about 15% of the 15-year record. The average significant wave height is about 7.5 ft. The two after-dredge bathymetry templates induced show wave changes are mostly less than 0.5 ft.

Figure 4-19 shows the model results for storm waves originating from SE, S, and SW. During Hurricane Matthew in 2016, significant wave height of 21 ft was observed offshore. Similar to the model results under more frequent normal wave conditions, the two after-dredge bathymetry templates could cause wave reduction leeward of the borrow area and wave increases on both east and west sides. The magnitude of wave change is mostly less than 1 ft in localized areas.
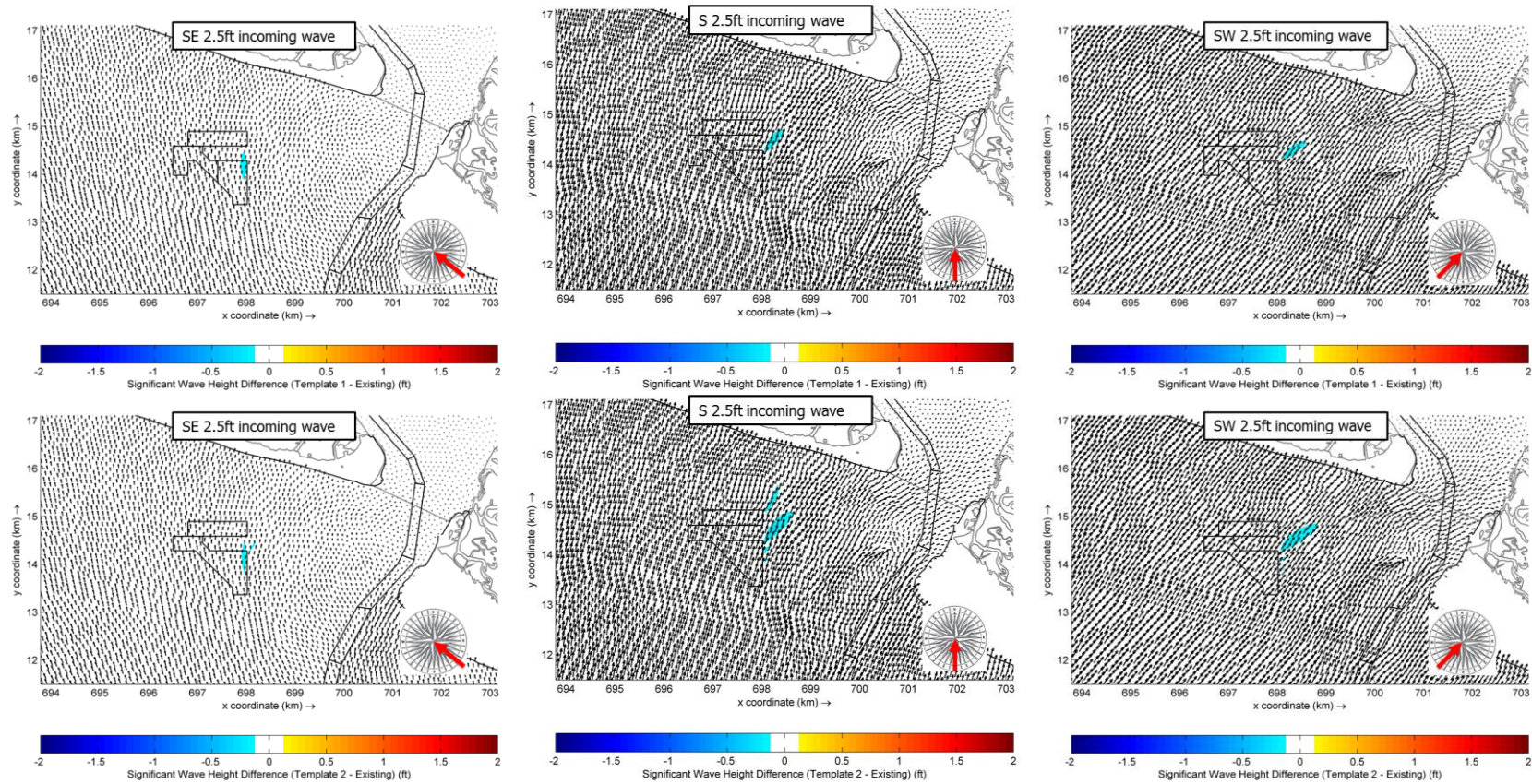
Figure 4-16: After-dredge bathymetry effects on waves between 0 – 3 ft with average height of 2.5 ft (top: Template 1; bottom: Template 2)
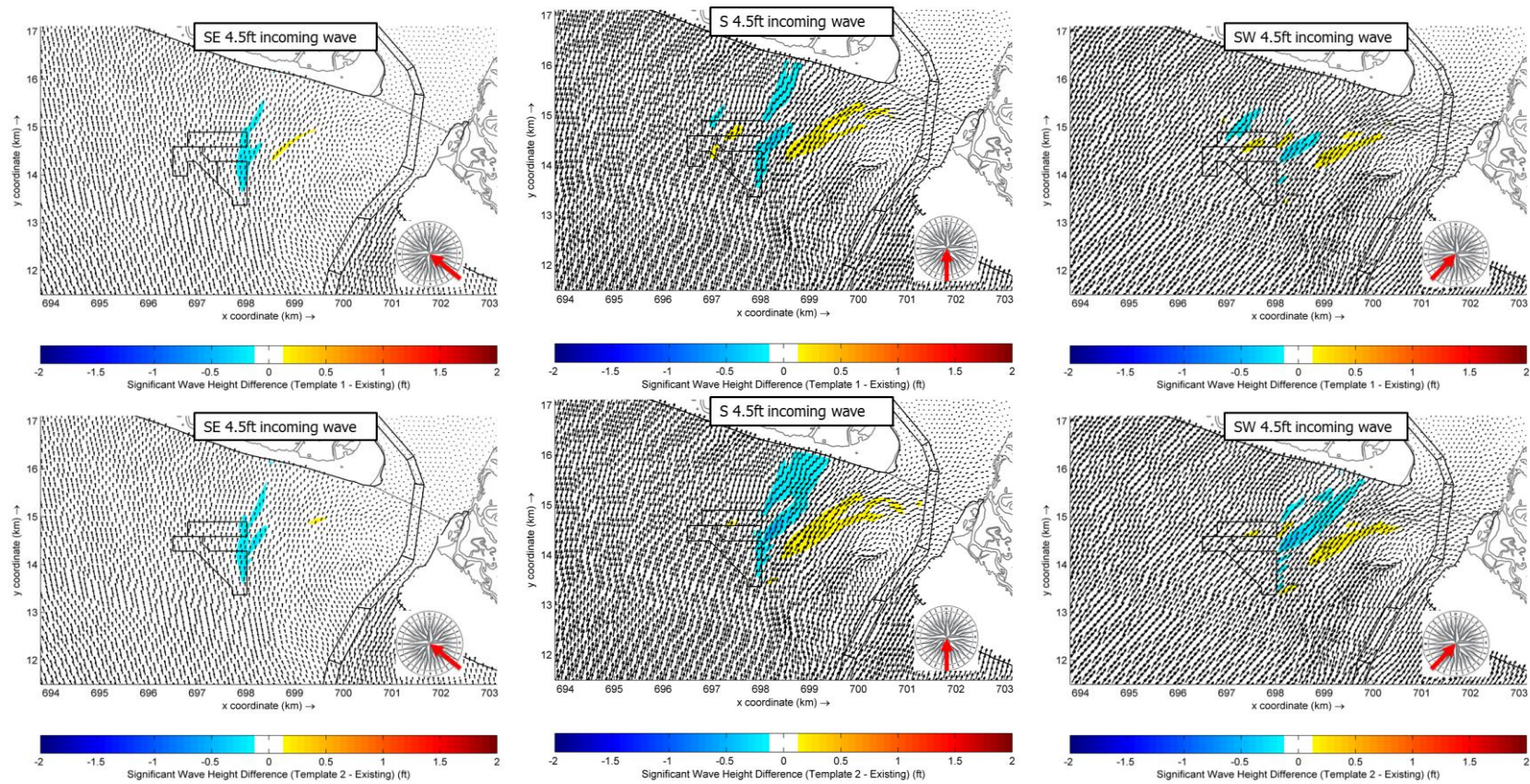
Figure 4-17: After-dredge bathymetry effects on waves between 3 – 6 ft with average height of 4.5 ft (top: Template 1; bottom: Template 2)
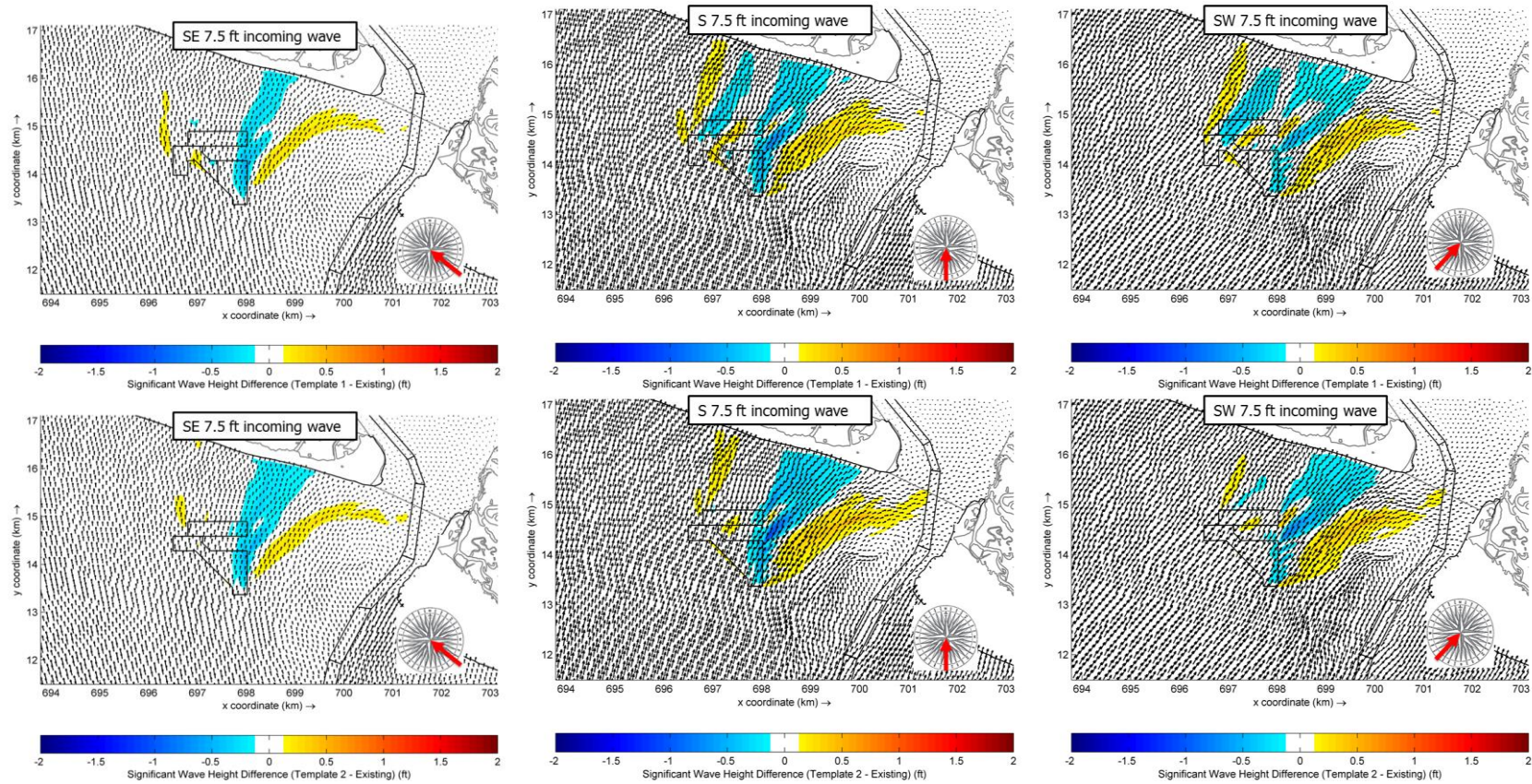
Figure 4-18: After-dredge bathymetry effects on waves between 3 – 6 ft with average height of 7.5 ft (top: Template 1; bottom: Template 2)
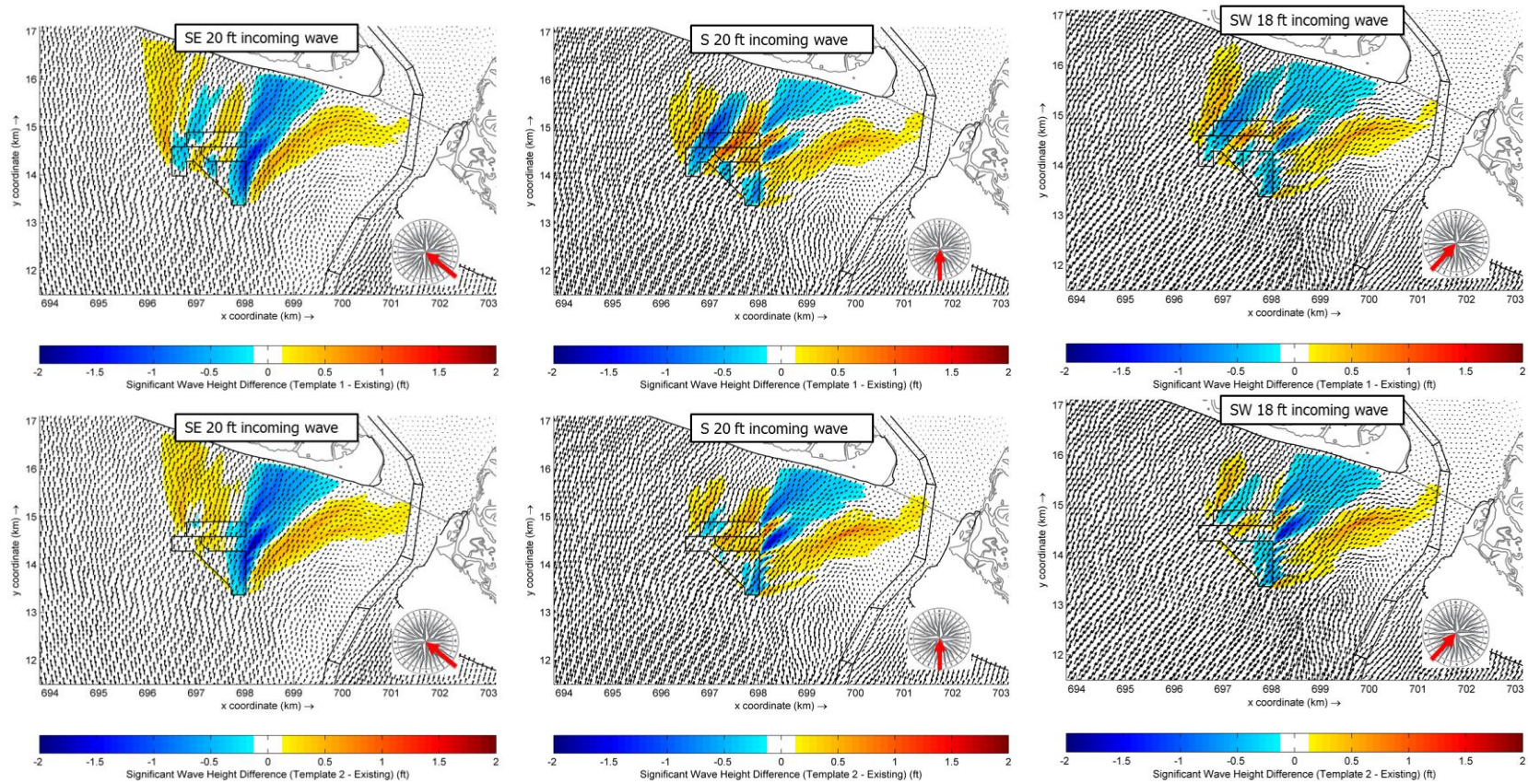
Figure 4-19: After-dredge bathymetry effects on storm waves comparable to Hurricane Matthew in 2016 (top: Template 1; bottom: Template 2)

4.3   SEDIMENT TRANSPORT

Based on the model results demonstrated in section 4.1.2, it is reasonable to conclude that the two after-dredge bathymetry templates have negligible effects on the residual tidal currents, and thus upon the associated sediment transport processes along the Caswell Beach shoreline due to tidal currents. Therefore, only wave induced sediment transport was considered for this analysis.

For each of the 86 representative wave conditions in Table 4-1, the wave induced longshore currents and associated sediment transport were estimated by coupling Delft3D-FLOW and Delft3D-WAVE modules using only the fine wave model grid for the existing and the two after-dredge bathymetric templates. There were no tide and wind inputs, and no morphology update. A uniform median sediment grain size of 0.25 mm was assumed. No sediment transport calibration effort was made due to lack of measured data.

The sediment transport rates through shore-normal transects along the Caswell Beach shoreline (Figure 4-20) were extracted from the model results under each wave condition; and were then subsequently weighted by the percent occurrence of each wave condition to formulate the average annual potential sediment transport. Modeled sediment transport inside the surf zone is greatly influenced by the imposed model bathymetry. Thus, the model results represent only the bathymetric condition constructed based on the available data sources listed in Table 2-1. In reality, the beach bathymetry tends to be smoothed out by waves. Since this sediment transport study is not a morphological model, the sediment transport results were smoothed through a 0.5 mile moving average.
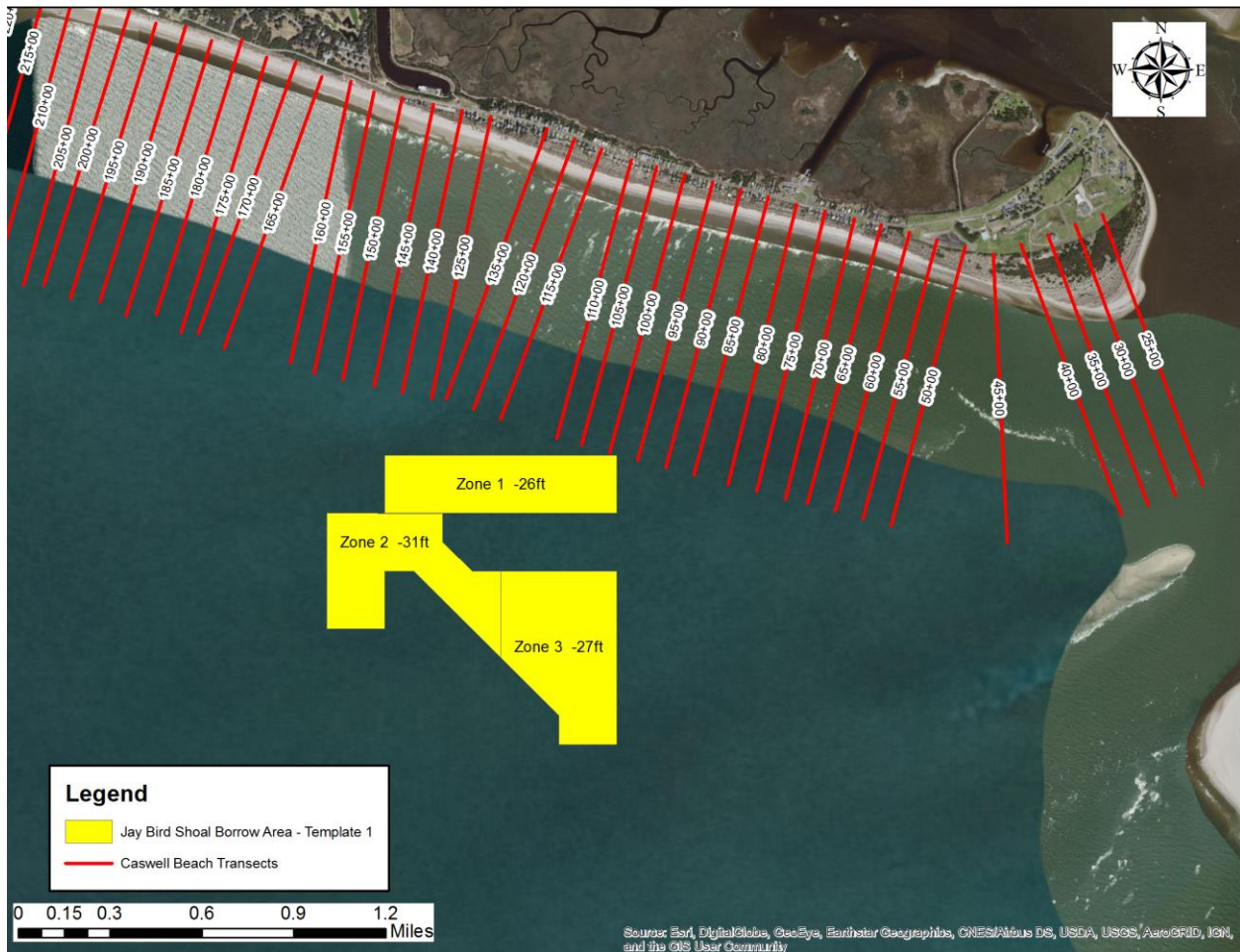
Figure 4-20: Caswell Beach transects

Figure 4-21 presents the modeled average annual "net" longshore sediment transport rates along the Caswell Beach shoreline for both the existing and the two after-dredge templates. Positive values represent westerly sediment transport direction. The model results indicate potential sediment transport rate reduction leeward of the borrow area, and potential sediment transport rate increases along both east and west shoreline segments away from the borrow area.

The net longshore sediment transport gradients along the Caswell Beach shoreline are shown in Figure 4-22. The net longshore sediment transport gradient is calculated as dQ/dx where dQ is the transport rate differential between neighboring transects and dx is the alongshore distance between transects. The transport gradient is a proxy to potential shoreline changes. Positive and negative values in Figure 4-22 indicate potential localized adjustments in shoreline accretion and erosion, respectively.

Based on the model results, it would appear that areas of concern for potential increases in shoreline erosion would be limited to discrete portions of Caswell Beach (between survey

transects 37+00 – 60+00 and 150+00 – 170+00). Potential effects on shoreline erosion in other areas seem to be minimal and some areas may experience increased shoreline accretion. Generally, both templates show results close to existing conditions, with some areas showing transport rates above and below existing conditions. There is no strong evidence to choose one template over the other given the model results, especially given that this is not a morphological model.   The modeled sediment transport inside the surf zone is greatly influenced by the imposed model bathymetry. Thus, the model results only represent the bathymetric condition constructed based on the available data sources.   There will be an additional 0.6 mcy beach compatible material available in Template 1.   For this reason, Template 1 was chosen for the Town of Oak Island's permit application for the 2019/2020 Renourishment Project. The Town of Oak Island will monitor the Caswell Beach shoreline for nine (9) years post-project to investigate any potential effects which might require mitigation.


Figure 4-21: Wave-induced net longshore sediment transports along Caswell Beach shoreline
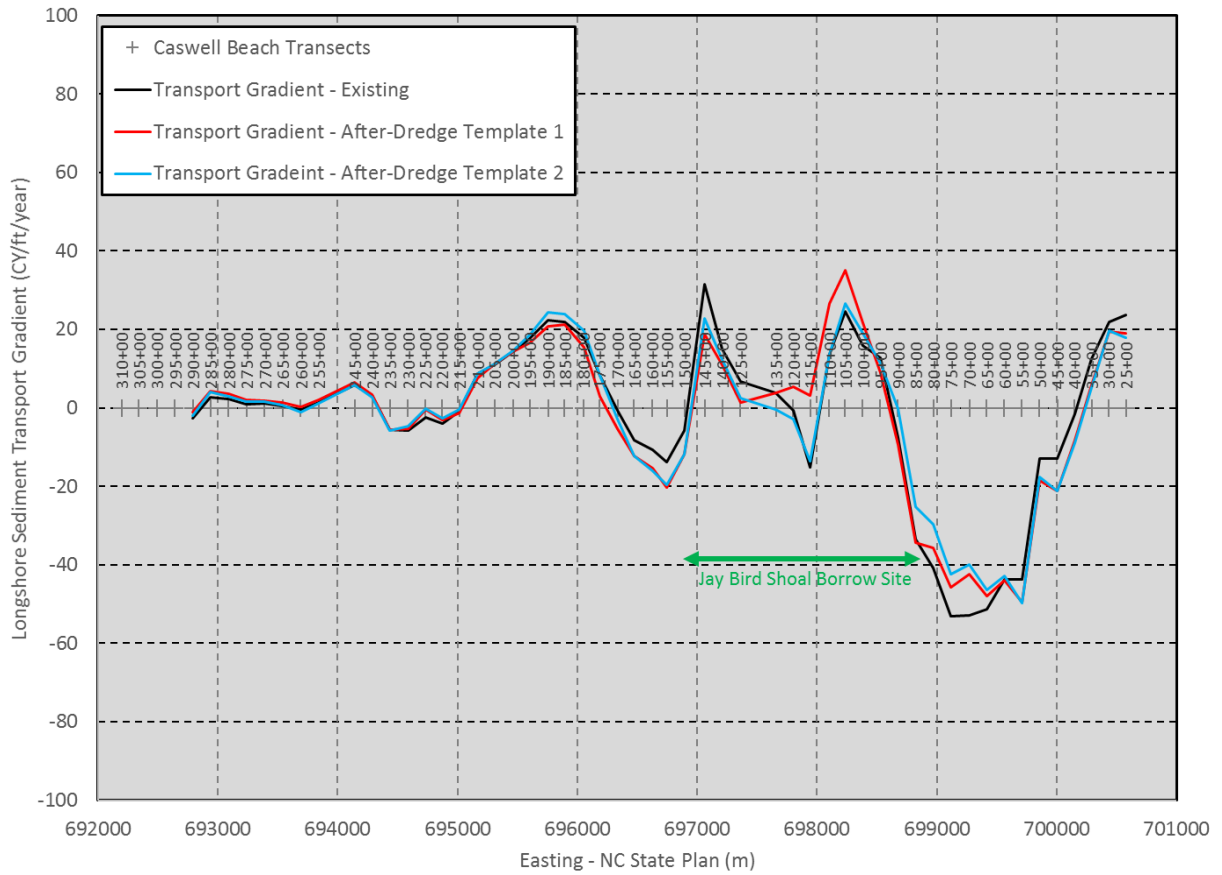
Figure 4-22: Longshore sediment transport gradients along Caswell Beach shoreline

5.   SUMMARY AND CONCLUSIONS

In order to investigate the potential effects of the Jay Bird Shoals borrow area identified for the 2019/2020 Renourishment Project on the neighboring shorelines of Caswell Beach and Bald Head Island, numerical models were developed for hydrodynamics, waves, and sediment transport using Deltares' Delft3D model suite. The hydrodynamics and wave models were successfully calibrated and validated against available observed water levels, currents, discharges, and wave data. Sediment transport calibration was not conducted, due to lack of measured data to calibrate against.

Tidal current, wave, and sediment transport modeling were performed for the existing and two after-dredge bathymetric templates. The maximum borrow area dredge scenarios were considered, i.e. assuming to remove the full 2.95/2.34 million cubic yards of available material identified as beach compatible in Template 1 and 2, respectively.   Only part of the material, 1.1 million cubic yards, will be dredged for the 2019/2020 Renourishment Project. Thus, within the proposed borrow area, the results from the Delft3D model are considered to be a conservative overestimate of the potential effects on tidal current and wave climates.

The model results were analyzed to determine potential effects of the two after-dredge bathymetric templates. The findings are:

- The two after-dredge bathymetric templates show that effects on tidal currents would be localized and small, which implies no significant effects upon sediment transport processes associated with tidal currents;

- The two after-dredge bathymetric templates could reduce waves leeward of the borrow area; however, it could slightly increase nearshore waves on both east and west sides of the borrow area in localized areas;

- and similarly, the two after-dredge bathymetric templates could reduce the wave-induced longshore sediment transports leeward of the borrow area but could also cause longshore sediment transport increases on shoreline segments both east and west sides of the borrow area.   The net effect of these changes could result in localized adjustments in shoreline erosion / accretion. Based on the model results, it would appear that most of the potential increases in shoreline erosion would be limited to discrete portions of Caswell Beach (between survey transects 37+00 –60+00 and 150+00 – 170+00).   Potential effects in other areas seem to be minimal. Generally, both templates show results close to existing conditions, with some areas showing transport rates above and below existing conditions. There is no strong evidence to choose one template over the other given the model results, especially given that this is not a

morphological model. The modeled sediment transport inside the surf zone is greatly influenced by the imposed model bathymetry. Thus, the model results only represent the bathymetric condition constructed based on the available data sources.

- Given that there will be an additional 0.6 mcy beach compatible material available in Template 1; this is the chosen scenario for the Town of Oak Island's permit application for the 2019/2020 Renourishment Project. The Town of Oak Island will monitor the Caswell Beach shoreline for nine (9) years post-project to investigate any effects predicted by the model which might require mitigation.

6. REFERENCES

Benoit, M., Frigaard, Peter, and H.A. Schäffer (1997) "Analyzing Multidirectional Wave Spectra", Proceedings of the 27th IAHR Congress, San Francisco, 10–15 August 1997, IAHR Seminar "Multidirectional Waves and their Interaction with Structures", Mansard, Etienne (ed.), Canadian Government Publishing, Benoit.

Deltares (2018a), "Delft3D-FLOW, Simulation of multi-dimensional hydrodynamic flows and transport phenomena, including sediments, User Manual".

Deltares (2018b), "Delft3D-WAVE, Simulation of short-crested waves with SWAN, User Manual".

Earle, M.D, K.E. Steele, and D.W.C. Wang (1999), "Use of advanced directional wave spectra analysis methods", Ocean Engineering, Volume 26, Issue 12, December 1999, Pages 1421–1434.

Egbert, Gary D., and Svetlana Y. Erofeeva (2002). "Efficient inverse modeling of barotropic ocean tides." Journal of Atmospheric and Oceanic Technology 19.2 (2002): 183-204.

RPS Evans-Hamilton (2017). "Cape Fear current, water Level and water quality study".

Willmott, C.J., S.G. Ackleson, R.E. Davis, J.J. Feddema, K.M. Klink, D.R. Legates, J. O'Donnell, and C.M. Rowe (1985), "Statistics for the evaluation and comparison of models", Journal of Geophysical Research, 90(C5), 8995–9005.